Title

Ecological relevance of abundant and rare taxa in a high-diverse elastic hypersaline microbial mat, using a small-scale sampling

Authors

Laura Espinosa-Asuar[1,*], Camila Monroy[1], David Madrigal-Trejo[1], Marisol Navarro[1], Jazmín Sánchez[1], Jhoseline Muñoz[1], Juan Diego Villar[2], Julián Cifuentes[2], Maria Kalambokidis[1], Diego A. Esquivel-Hernández[1], Mariette Viladomat[1], Ana Elena Escalante-Hernández[3] , Patricia Velez[4], Mario Figueroa[5], Santiago Ramírez Barahona[4], Jaime Gasca-Pineda[1], Luis E. Eguiarte[1]and Valeria Souza[1,*].

Affiliations

[1]Departamento de Ecología Evolutiva, Instituto de Ecología, Universidad Nacional Autónoma de México, AP 70-275, Coyoacán 04510, Ciudad de México, México

[2]Pontificia Universidad Javeriana, Bogotá D.C., Colombia

[3]Laboratorio Nacional de Ciencias de la Sostenibilidad, Instituto de Ecología, Universidad Nacional Autónoma de México, AP 70-275, Coyoacán 04510, Ciudad de México, México, City, México

[4]Departamento de Botánica, Instituto de Biología, Universidad Nacional Autónoma de México, Coyoacán 04510, Ciudad de México, México

[5]Facultad de Química, Universidad Nacional Autónoma de México, Coyoacán 04510, Ciudad de México, México

*corresponding authors:

lauasuar@ecologia.unam.mx; souza@unam.mx

Abstract

We evaluated the microbial diversity and metabolomic signatures of a hypersaline elastic microbial mat from Cuatro Ciénegas Basin (CCB) in the Chihuahuan Desert of Coahuila, México. We collected ten samples within a small scale (1.5-meters transect) and found a high microbial diversity through NGS-based ITS and 16S rRNA gene sequencing. A very low number of taxa were abundant and shared between all sites, whereas the rare biosphere was more phylogenetically diverse (FPD index) and phylogenetically disperse (PSC index) than the abundant taxa for both analyzed libraries. In regard to potential biotic interactions (Pearson analysis), there were more positive correlations than negative. We also found a distinctive metabolomic signature for each sample and were able to tentatively annotate several classes of compounds with relevant biological properties. Together, these results reveal cohesive, diverse and fluctuating microbial communities, where abundant and rare taxa appear to have different ecological roles.

Kewords: biotic interactions, Cuatro Ciénegas Coahuila, metabolomic analyses, microbial communities, phylogenetic diversity, rare biosphere.

Introduction

Microbial mats are tightly interacting communities, usually self-sustaining, that are horizontally stratified with multilayered biofilms embedded in a matrix of exopolysaccharides binding cells and inorganic substances together (Bolhuis et al., 2014; Prieto-Barajas et al., 2018; Stolz, 2000). These stratified structures, as well as stromatolites, are the oldest communities found in the fossil record, informing our understanding of ancient metabolic interactions (Gutiérrez-Preciado et al., 2018; Nutman et al., 2016).

Although modern microbial mats and stromatolites are geographically widespread (Gerdes, 2010), their distribution is restricted to extreme environmental conditions where multicellular algae and grazing organisms cannot grow (Bebout et al., 2002). One such site, with a high diversity of microbial mats and stromatolites, is the desert oasis of the Cuatro Ciénegas Basin (CCB), found in the Chihuahuan Desert of the

state of Coahuila in northern México. This small site (150,000 km^2) is extremely biodiverse – in particular for microbes (Souza, Eguiarte, et al., 2018) – and is considered of international importance by the RAMSAR convention (www.ramsar.org). CCB is characterized by an imbalanced stoichiometry (i.e., very low concentration of phosphorus) (Elser et al., 2005, 2006; Papineau, 2010; Planavsky et al., 2010), which appears to be a strong selective pressure driving microbial lineages to adapt locally and form extremely cohesive and co-adapted microbial communities (Souza, Eguiarte, et al., 2018). The uniqueness of microbial life in CCB -- characterized as an "Astrobiological Precambrian Park" (Souza et al., 2012) -- is reflected in the presence of ancient marine lineages (Rebollar et al., 2012; Souza et al., 2006; Souza, Eguiarte, et al., 2018), rich prokaryotic communities (López-Lozano et al., 2013; Pajares et al., 2012, 2013; Souza, Olmedo-Álvarez, et al., 2018) , and diverse fungal (Velez et al., 2016) and viral communities (Taboada et al., 2018), as well as a high microbial diversity within microbial mats and stromatolites (Bonilla-Rosso et al., 2012; De Anda et al., 2018; Peimbert et al., 2012).

In March 2016, we discovered an outermost elastic layer microbial mat in CCB, which enables the formation of dome-like structures under wet conditions (Fig. 1).

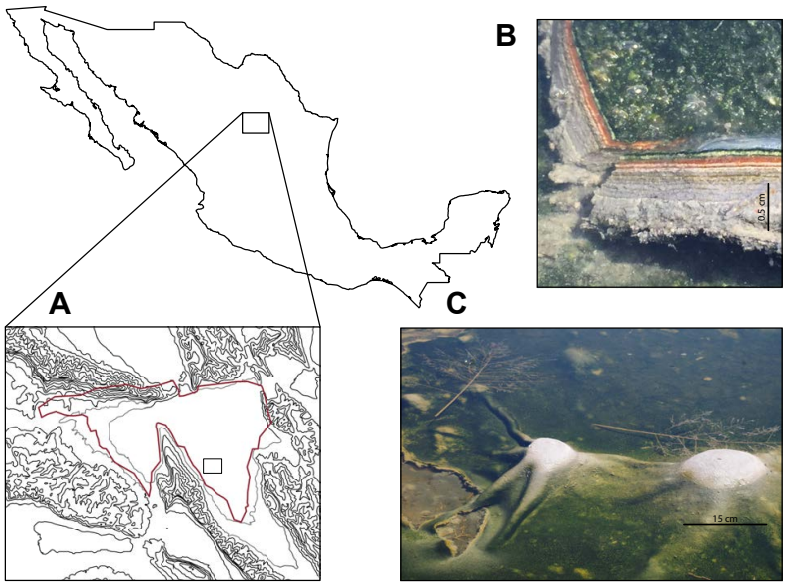

Figure 1

(A) The Cuatro Ciénegas Basin within México, and geographic location of Archaean Domes in Pozas Azules Ranch. (B) Detail of an Archaean Domes slice. (C) Domes when the sampling was conducted (note the size scale). Photos by David Jaramillo.

The internal microbial layer, insulated by an outer aerobic community, thrives under an anaerobic environment, rich in methane and hydrogen sulfide, and small volatile hydrocarbons that recreate the atmosphere of the Archaean Eon, hence we named these mats “Archaean domes” (Medina-Chávez et al., 2020). Similar types of elastic mats have previously been described in marine tidal zones, although their formation is relatively rare (Gerdes et al., 1993).

Given their functional richness, microbial mats are ideal systems for analyzing the role of microbial interactions in maintaining community structure under extreme conditions (Paerl & Yannarell, 2010; Prieto-Barajas et al., 2018). In this sense, there are three approaches that can improve our understanding of biotic interactions and processes at an evolutionary scale (Mayfield & Levine, 2010) for microbial mat communities. First, determine the phylogenetic diversity of communities under extreme environmental conditions where, for example, abiotic filtering and competitive exclusion have been reported as drivers of phylogenetic clustering (Goberna et al., 2014;). Second, investigate the ecology of microbial subcommunities, such as those of rare taxa, a less-studied topic than the whole community (Liu et al., 2019) but important to explore for their potential contribution to ecological processes (Jia et al., 2018). Third, analyze the metabolomics of communities, which is one of the functional expressions of diversity and an underexplored aspect of microbial communities that can help complete our understanding of the observed diversity. Moreover, metabolomics can also elucidate ecological aspects (Sardans et al., 2011) that help uncover the reciprocal interactions between ecology and evolution, known as eco-evolutionary feedbacks (D. M. Post & Palkovacs, 2009).

In this study, we evaluated the microbial diversity, the rare biosphere, and its metabolomic signature within this elastic hypersaline microbial mat from CCB, across ten samples collected within a 1.5-meter transect. Specifically, we aimed: 1) to explore microbial diversity analyzing amplicons of the 16S rRNA and ITS regions,

109 2) to determine whether rare and abundant taxa are phylogenetically structured; 3)
110 to evaluate microbial metabolomic signatures as an approximation to eco-
111 evolutionary feedbacks; and 4) to approximate biotic interactions.
112
113 **Results**
114 ***Microbial taxonomic composition***
115 16S rRNA gene and ITS libraries revealed the occurrence of different microbial
116 lineages, as genera composition showed (Fig. 2).

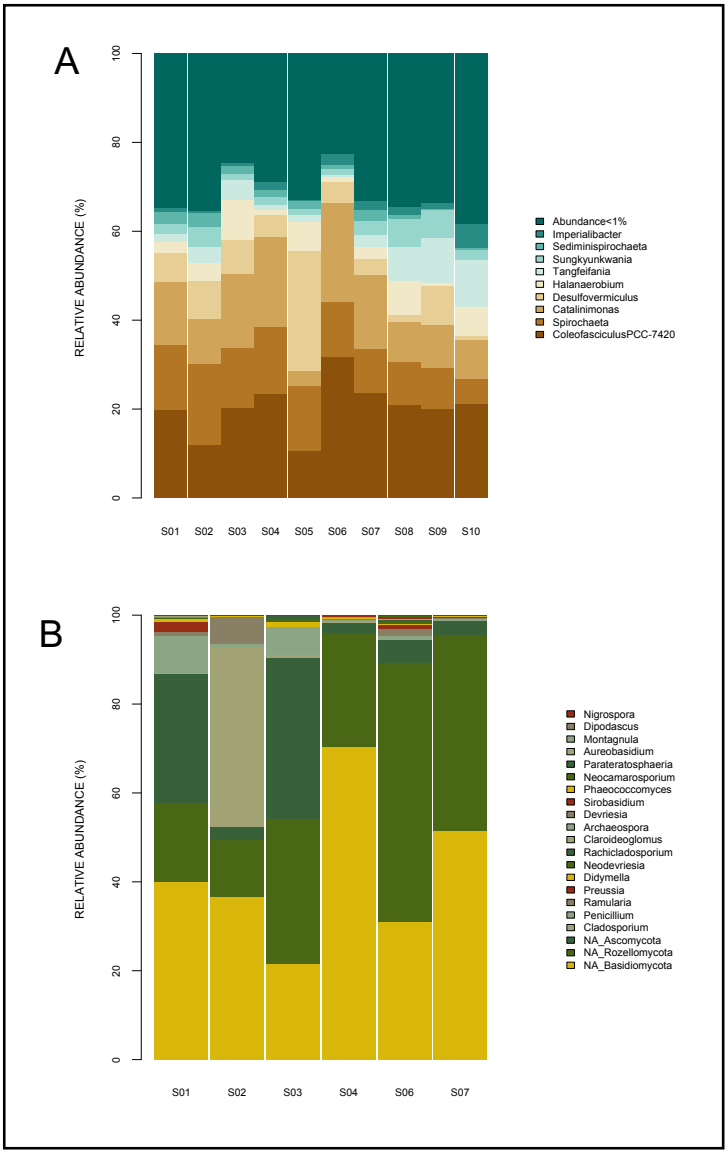

Figure 2
Genera relative abundance of taxa in Archaean Domes, Cuatro Ciénegas Basin sample. A) Bacteria (only showed the most common taxa, more than 1% of diversity) B) Fungi (using Merge database, only fungal ASVs. NA is for ASVs that were not assigned to any genera, but phylum only).

124 Overall, 40 prokaryote phyla were detected from the 16S rRNA gene libraries (Suppl.
125 Fig. 1A), and a total of 6,063 different ASVs were found, with a proportion of 11.8%
126 of unclassified reads (Suppl. Table 2). Bacteroidetes was the most abundant phylum,
127 representing around 23% of the prokaryotic diversity in the samples, followed by
128 Proteobacteria with ≈ 19% and Cyanobacteria with nearly 18%. Spirochaetes and
129 Chloroflexi represented ≈ 8% and ≈ 4% of the prokaryotic diversity, respectively.
130 Nearly 2% were Firmicutes, Patesibacteria and Halanaerobiota (Suppl. Fig. 1A).
131 A total of 410 genera of Bacteria were detected in the 10 sampled sites (S1-S10) at
132 a 1.5 m-scale. From those, only 9 genera were abundant (representing ≈ 70% of
133 total abundance, Fig. 2 A): *Coleofasciculus* (or *Microcoleus*), *Spirochaeta*,
134 *Catalinimonas*, *Desulfovermiculus*, *Halanaerobium*, *Tangfeifania*, *Sungkyunkwania*,
135 *Sediminispirochaeta* and *Imperialibacter*. The remaining 401 genera can be
136 classified as rare biosphere, with ≈ 30% of total abundance (less than 1% each, Fig.
137 2 A). Moreover, 28 ASVs of Archaea were obtained using our 16S primers,
138 comprising two phyla, Woesearchaeota and Euryarchaeota (Suppl. Fig. 1a).
139 Halobacteria class was the most abundant, and we detected 4 genera: *Halovivax*,
140 *Halorubrum, Halorussus* and *Haloasta* (Suppl. Table 2).
141 For the ITS region libraries, we successfully obtained reads for six of the sampled
142 sites (S1 to S4, S6 and S7). For the Forward-Only ITS database, we detected 923
143 different ASVs. The majority of the classified reads belong to Alveolata protists (77%,
144 Suppl. Fig. 1B), followed by Fungi (11%) and Viridiplantae (8%); Metazoa, Protista,
145 Amoebozoa, Rhodoplantae, Chromista and Stramenophila comprised the remaining
146 4%. Unassigned taxa were 50% of all reads (Suppl. Table 2). The majority of ASVs
147 within Forward ITS database could not be accurately classified at lower taxonomic
148 categories, particularly for three common ASVs (ASV0 (unclassified), ASV1
149 (Ciliophora) and ASV2 (Ciliophora)), which comprise nearly 70% of the abundance
150 in ITS reads for all sites. Using Merge ITS ASVs database for a better taxonomic
151 assignment, Fungal ASVs comprising 18 genera were detected, with phyla
152 Ascomycota, Basidiomycota and Rozellomycota present in all samples (Fig. 2B).
153
154

155 ***Alpha and beta diversity***

156 Rarefaction curves (Suppl. Fig. 2A and 2B) showed similar results for both the
157 Forward-Only ITS region libraries (S1, S2, S3, S4, S6, S7), and 16S rRNA gene
158 libraries, as all sites reached an asymptote, suggesting an adequate sampling effort.
159
160 Only 183 ASVs (3% of the diversity) were shared between all sites for 16S rRNA
161 gene libraries (Fig. 3A), forming a very small core, but comprised 72.4% of all reads
162 (composed of twenty-one phyla), while most of the ASVs were unique to a specific
163 site or shared between two or three sites. For ITS libraries, the 56 shared ASVs (6%)
164 comprised 94.7% of all reads (Fig. 3B).
165
166
167

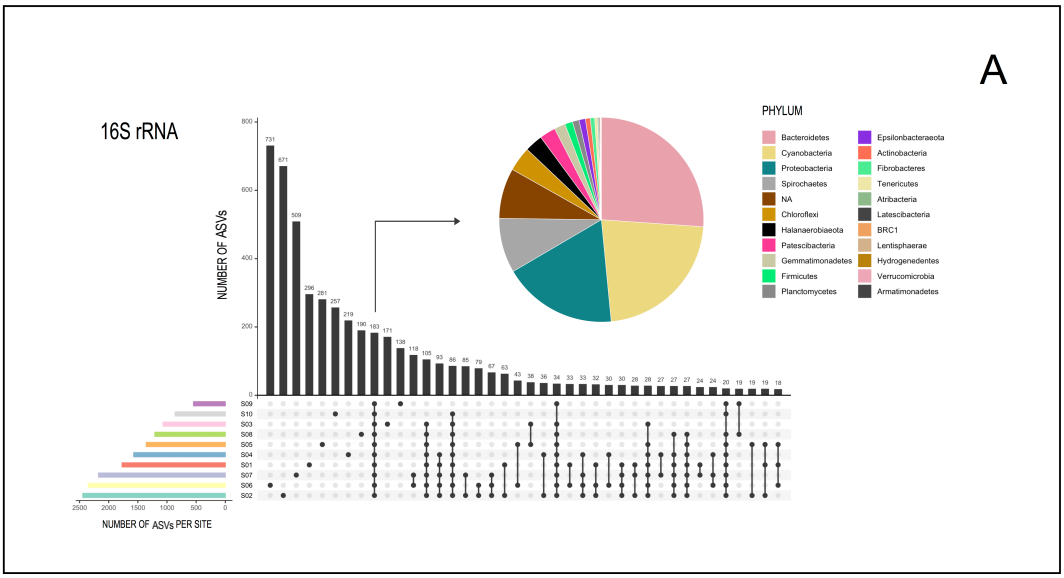

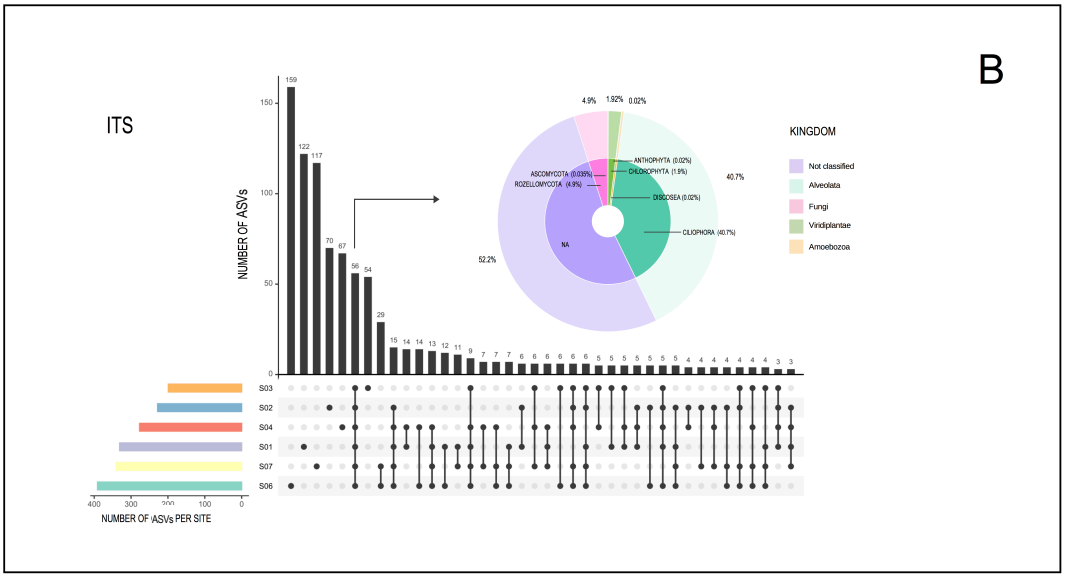

Figure 3
Graphic representation of shared ASVs within Archaean Domes mats sampling sites. Number of shared ASVs is represented by black bars, showing the exact number on the top. Dots below bars denote sites where those ASVs are shared, and lines joining dots indicate the shared sites. Colored bars at bottom left of the main figure are for ASVs number within each site. Pays show taxonomy of shared ASVs within all sites (a few but abundant ASVs core). (A) 16S Archaea and Bacteria, rRNA gene database, (B) Fungi and other Eucarya, Forward-Only ITS database.

178 16S rRNA ASVs alpha diversity (Table 1) ranged from 2470 expected ASVs
179 according to Chao1 in S2 (Shannon = 7.4, highest Shannon index value), to 544
180 expected ASVs in S9 (Shannon = 6.1). In the case of the ITS region libraries
181 (Forward-Only ITS database), the most ASV Chao1 diversity for Eukarya was S6
182 with 393 expected ASVs and a Shannon diversity of 2.5; S3 had the lowest Chao1
183 diversity, with 199 expected ASVs, but this site had the highest Shannon value of 3
184 (Table 1).

ITS region						
	α diversity			Phylogenetic diversity		
Sample	Observed	Chao	Shannon	Faith PD	Faith PD rare	Faith PD abundant
1	322	322	1.827	86.309	42.596	18.161
2	226	226	2.713	60.622	40.846	14.516
3	199	199	3.062	47.289	30.370	14.774
4	270	275	1.783	83.008	51.513	16.287
6	383	393	2.501	131.435	75.352	28.794
7	337	344	2.008	114.983	60.352	18.865

185

16S rRNA						
	α diversity			Phylogenetic diversity		
Sample	Observed	Chao	Shannon	Faith PD	Faith PD rare	Faith PD abundant
1	1761	1773.203	6.863	544.704	290.491	44.159
2	2399	2470.398	7.402	789.807	368.430	84.442
3	1068	1071.318	6.256	211.745	156.204	20.064
4	1564	1568.664	6.499	500.787	259.828	40.627
5	1344	1358.842	6.882	220.536	172.299	21.557
6	2345	2353.855	6.301	851.168	302.103	131.337
7	2156	2172.218	6.838	759.536	328.238	97.486
8	1195	1217.568	6.487	205.987	139.839	22.798
9	544	544	6.126	160.368	94.201	18.577
10	828	875.634	5.115	283.017	148.655	36.514

186
187 Table1

188 Alpha diversity indices for 16S rRNAgene and Forward-Only ITS region databases
189 from Archaean Domes CCB microbial mats.

190 Paired beta bacterial diversity among microbial mat samples for both the 16S rRNA
191 gene and ITS region databases ranged from 0.2 to 0.7 for the Bray-Curtis diversity
192 values and 0.3 to 0.7 according to the Jaccard-1 values (Suppl. Fig. 3 A and B). For
193 both indexes, S10 is different from the rest of the 16S rRNA gene libraries, and S1,
194 S2, S4, S6, S7 were associated in a cluster. In the ITS libraries, there are two main
195 clusters (S1, S2 and S4; S3, S6 and S7). A significant geographic pattern in the
196 Mantel test (p=0.0402) was found for Jaccard-1 of the 16S library, however we did
197 not find significant values based on geography for ITS libraries for either Jaccard-1
198 or Bray-Curtis.
199
200 *Phylogenetic Diversity*
201 For both libraries, Faith Phylogenetic Diversity showed that rare ASVs were more
202 diverse than abundant ASVs (Table 1), and Phylogenetic Species Clustering (PSC)
203 measures showed that abundant ASVs were clustered within phylogeny, while rare
204 ASVs were disperse (Fig. 4 A and B).

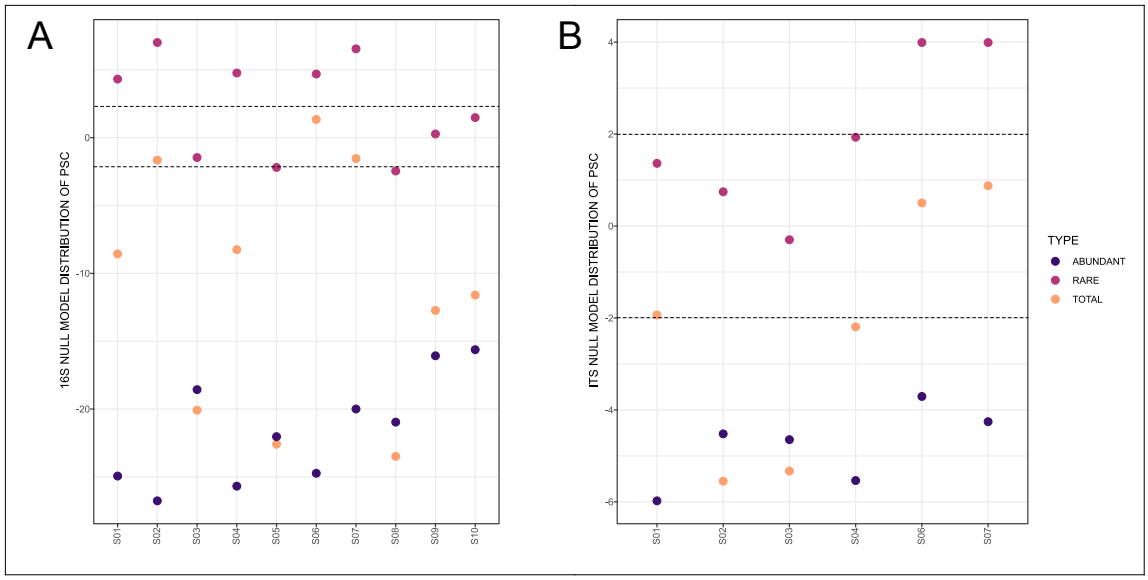

205
206 Figure 4
207 Graph representing null model distribution of Phylogenetic Species Clustering
208 (nmdPSC) values for all community, abundant and rare taxa from 16S rRNA
209 database (A) and Forward-Only ITS database (B). Dotted lines are showing
210 nmdPSC significant values: > +2 is consistent with a sample that had more
211 phylogenetic overdispersion than expected by chance alone, and nmdPSC value <
212 -2 indicates more phylogenetic clustering than expected by chance alone; values in

the range +2 and -2 had a null model distribution. nmdPSC values are reported in Suppl. Table 5.

Approximation to biotic interactions: Pearson analysis

In order to identify potential biotic interactions within the dominant taxa from the three domains of life within the Archaean Domes, we calculated Pearson correlations between ASVs (Fig. 5).

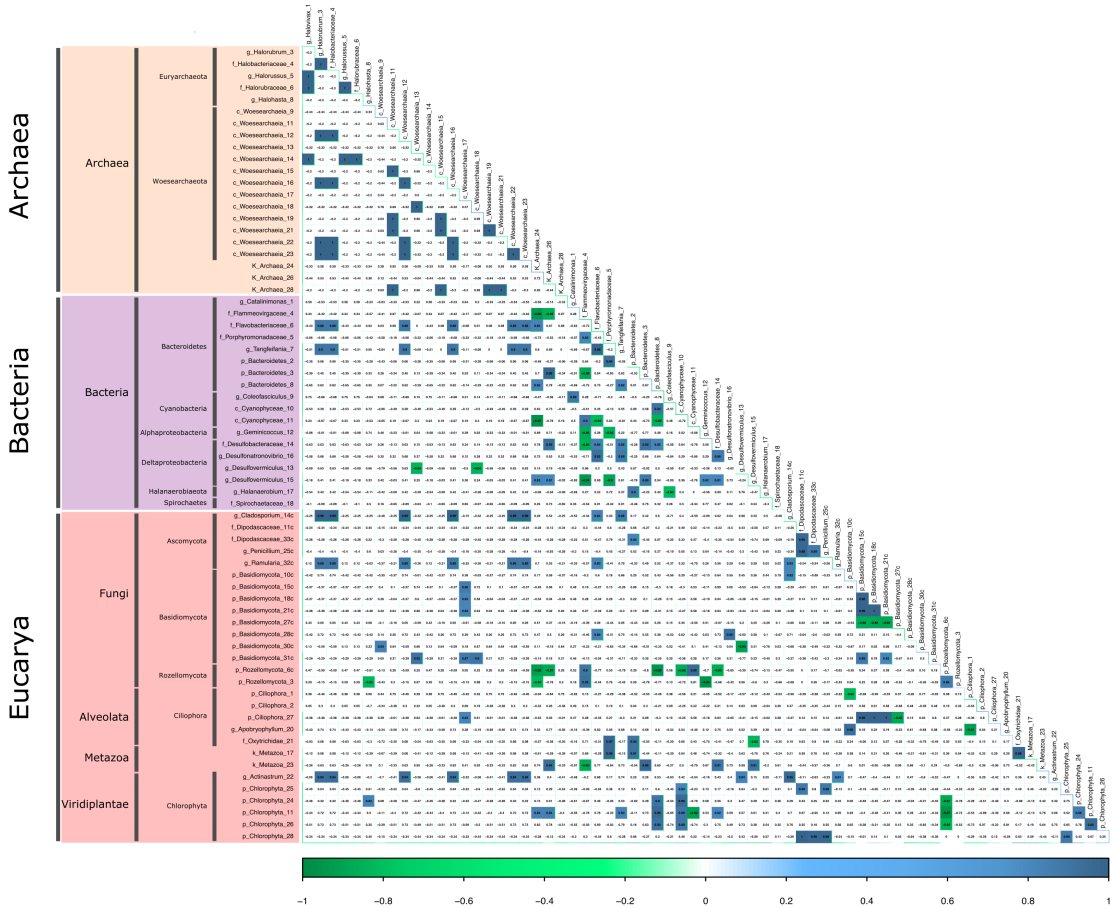

Figure 5
Pearson correlation analysis within the most common (i.e., involving more than 1% of diversity) Bacteria, and all genera of Archaea and Fungi (from Merge ITS database). Colored squares are for significant correlations (P≤0.05), blue for positive ones and red for negatives.

We analyzed the most abundant ASVs (above 1%) from the 16S rRNA gene libraries and both ITS databases, along with 22 Archaea ASVs. We observed that most of the negative co-occurrence correlations are associated with Bacteria, in particular

230 the Bacteroidetes phylum. Within the complete correlation matrix, we observed 22
231 negative co-occurrence correlations, along with 9 for Archaea,14 for Fungi, and 6 for
232 Eukarya (see Suppl. Table 3 for interaction counts). In addition, we observed that
233 Archaea-Archaea correlations (Fig. 5) were mostly positive (80), the majority of them
234 enclosed within Archaea ASVs (32), whereas Eukarya-Eukarya interactions had the
235 fewest positive correlations (4). Remarkably, in the cross-kingdom fungal
236 interactions, most of the negative fungal correlations (8 of 14) were observed in
237 Rozellomycota.
238
239 ***Metabolomic profile***
240 We found a wide range of metabolites based on heatmap and GNPS molecular
241 networking analysis (Fig. 6 and Suppl. Fig. 4 A&B).

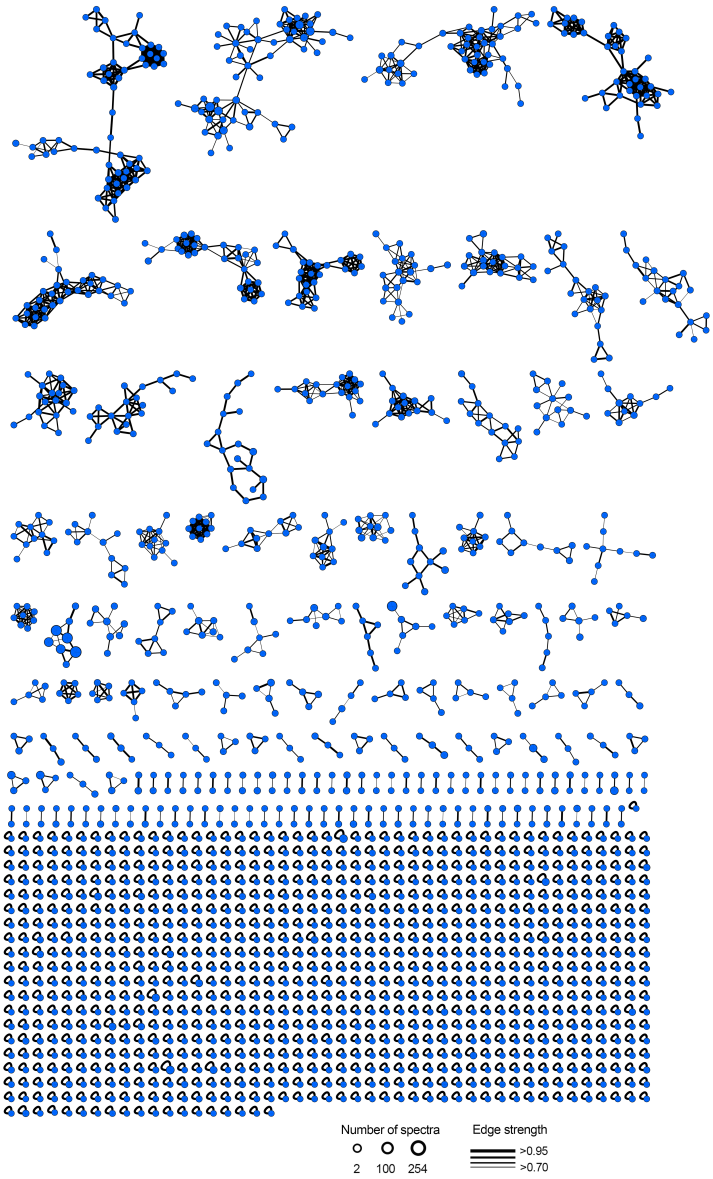

Figure 6
Molecular network of soil samples grouped metabolite features into 140 chemical families. Each node in the network represents one metabolite feature. Nodes connected to each other are structurally-related (cosine MS^2 similarity score ≥0.7).

Untargeted metabolomics analysis of microbial communities is complicated, due to the complexity and heterogeneity of this matrix and the scarcity of the secondary metabolites extracted. The 1,341 molecular features at unique retention times (Suppl. Fig. 4 A&B) shared several common regions across all samples, allowing us

252 to group them into three main clusters (cluster 1, samples 3-5 and 10; cluster 2,
253 samples 1, 2 and 6; and cluster 3, samples 7-9, Suppl. Fig. 4B). We found highly
254 heterogeneous metabolic profiles in all samples, and no significant associations
255 were observed between metabolite features and ITS or 16SrRNA abundance
256 matrices.
257 On the other hand, GNPS molecular networking analysis grouped the metabolite
258 features in 18,547 nodes distributed into 83 chemical families (sub-networks) of ≥3
259 members, 57 families of two metabolite features, and 875 singletons (Fig. 6).
260 Detected compounds in the GNPS and detailed metabolomic analysis of the main
261 ions observed in LC-MS/MS data, focused in microbial metabolites, allowed us to
262 tentatively identify several secondary metabolites that passed our quality criteria (≤
263 5 ppm mass error; Suppl. Table 4 and Fig. 7).

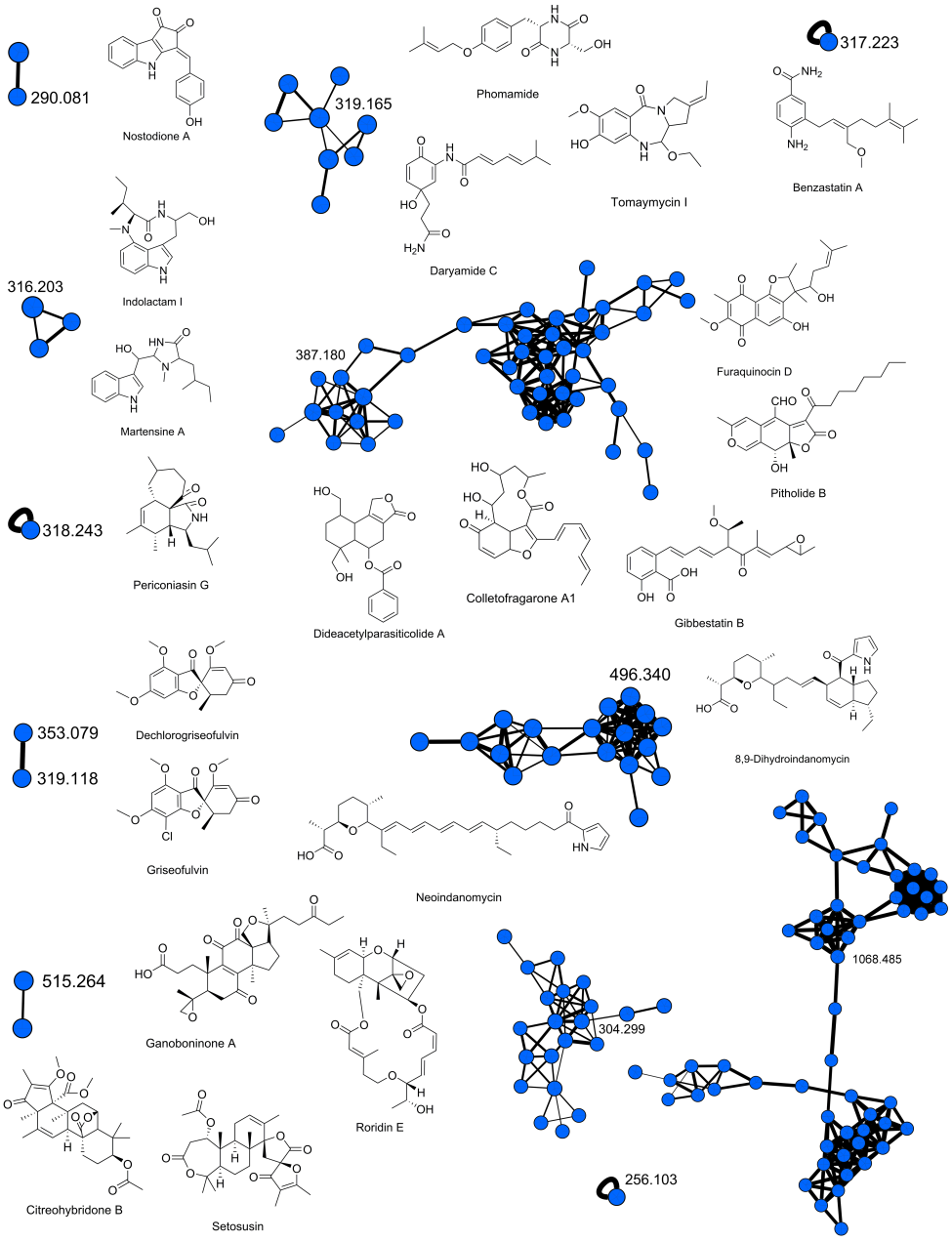

Figure 7
Structures of microbial metabolites tentatively annotated in samples S1-S10 (≤ 5 ppm mass error).

Discussion

Microbial composition at a microscale

Our study revealed a remarkably high microbial diversity within a 1.5 m scale in an elastic microbial mat located at an extreme site. Altogether, we found 40 prokaryotic phyla, including 410 genera of Bacteria and 4 of Archaea, as well as 18 Fungal genera (Fig. 2 and Suppl. Fig. 1).

Bacteria

The bacterial phyla (Suppl. Fig. 1) detected in our study site are common components of hypersaline microbial mats (Bolhuis et al., 2014; Visscher et al., 2010): Bacteroidetes, Proteobacteria, Cyanobacteria, Chloroflexi, and Firmicutes, among other abundant phyla, which are similar at this broad taxonomic level to other sites in CCB (Bonilla-Rosso et al., 2012; Breitbart et al., 2009; De Anda et al., 2018; Nitti et al., 2012). As expected from a microbial mat, a primary producer was present and abundant in all of our samples: *Coleofasciculus* (*Microcoleus)* (Fig. 2), a filamentous nitrogen-fixing cyanobacteria genus well-adapted to saline conditions (De Wit et al., 2013; Ramos et al., 2017) that has been reported in Guerrero Negro microbial mats (Des Marais, 2010; Wong et al., 2016). We also found the abundant taxon *Catalinimonas,* which is a halophilic Bacteroidetes marine genus (Choi et al., 2013) that has not been previously reported in microbial mats. Another common taxon in our samples is the *Spirochaeta* genus (Bolhuis et al., 2014; Margulis et al., 2006), an anaerobic chemo-organotrophic taxa abundant in hypersaline marine mats (Ben Hania et al., 2015). Interestingly, the *Spirochaetes* phylum has not been detected previously in any CCB mats (Bonilla-Rosso et al., 2012; de Anda et al., 2018; Peimbert et al., 2012). We also observed *Desulfovermiculus*, a sulfate-reducing Deltaproteobacteria, and *Halanaerobium*, a thiosulfate-reducing Firmicute that is halophilic and can form spores (Liang et al., 2016), both of which are common genera in marine microbial mats (Bolhuis et al., 2014).This suggests that this shallow salty pond could be more similar to marine lineages than other sites in CCB (see Rebollar et al., 2012; Souza et al., 2006, 2018).

300 Previous metagenomic analysis from a mat in Churince within CCB reported 1,431
301 OTUs (de Anda et al., 2018) – four times less diverse than the Archaean Domes
302 (6063 ASVs). Other studies within CCB, also with complete metagenomes, retrieved
303 250 expected OTUs using 31 core genes (Bonilla-Rosso et al., 2012). Therefore, it
304 is possible that using high coverage 16S tags may reveal a hidden high-diverse rare
305 biosphere in these microbial mats.
306 Regarding the high diversity within the Archaean Domes and comparing it with other
307 microbial mats (since ASVs and OTUs are reported providing similar ecological
308 results (Glassman & Martiny, 2018)), Cardoso et al. (2019) reported 977 OTUs in
309 marine microbial mats, and Wong et al. (2015) found 4800 OTUs in Shark Bay, which
310 are considered some of the most diverse microbial mats worldwide.
311
312 *Archaea*
313 In a recent metagenomic study of the Archaean Domes (Medina-Chávez et al.,
314 2020), Archaea taxa formed a constant core that is more diverse than any other site
315 within or outside of CCB. In those metagenomes, Archaea represented nearly 5% of
316 the total reads, accounting for 230 ASVs.
317 In our data, by using 16S rRNA gene amplicons, we only detected two main phyla,
318 as expected given the nature of the amplified region (Suppl. Fig. 1 and Suppl. Table
319 2). These were Woesearchaeota, a mainly halophilic phylum and potentially
320 syntrophic within methanogens (Liu et al., 2018; Ortiz-Alvarez & Casamayor, 2016),
321 and Euryarchaeota, within which we found four halophilic genera: *Halovivax*,
322 *Halorubrum, Halorussus* and *Haloasta*, all of them previously reported within saline
323 habitats and sediments (McGonigle et al., 2019; Zaitseva et al., 2018). The
324 metagenomic data (Medina-Chávez et al., 2020) and the 16S rRNA gene amplicons
325 were sampled from the same pond at different times and space, and both showed
326 lineages common to hypersaline habitats.
327
328 *Fungi*
329 Fungal members represent a diverse and common component of hypersaline water
330 columns and mats (Cantrell et al., 2013) and have been suggested to play a role in

331 the degradation of EPS (exopolymeric substances) (Cantrell & Duval-Pérez, 2013).
332 Our results suggest that unidentified uncultured members of the Ascomycota and
333 Rozellomycota comprise the core mycobiota of the analyzed mats, as they occurred
334 across all the samples (Fig. 3B). In addition, it is feasible that these abundant
335 heterotrophs occupy a unique niche within the micro-scale of microbial mats, where
336 they can degrade the abundant EPS produced in the CCB microbial mats (Breitbart
337 et al., 2010; De Anda et al., 2018; Peimbert et al., 2012). In particular, halotolerant
338 taxa such as members within the genera *Aspergillus*, *Penicillium*, and *Nigrospora*
339 have been repeatedly reported in microbial mats at other locations (Cantrell et al.,
340 2013; Cantrell & Duval-Pérez, 2013), evidencing their adaptation to extreme
341 conditions. Thus, it appears that, similar to other microbial mats, fungal members
342 occupy a unique niche within the micro-scale of the Archaean Domes (Cantrell et
343 al., 2011).
344
345 *Other eukaryotes*
346 The overall diversity of protists in the Archaean Domes is comparable to the diversity
347 observed in other microbial mats (329 ASVs, Suppl. Table 2). For example, Saghaï
348 et al. (2017), reported nearly half of the 586 18S rRNA OTUs they analyzed as
349 Protozoa in a saline shallow pond mat in Chile, while ≈ 500 eukaryotic 18S rRNA
350 OTUs were observed in mats from hydrothermal vents in Guaymas Basin (Pasulka
351 et al., 2019), where half of them were likewise classified as Protozoa taxa. More than
352 1500 eukaryotic 18S rRNA OTUs were detected in microbialites in Highborne Cay,
353 Bahamas, and Hamelin Pool (Shark Bay), Australia (Edgcomb et al., 2014), with also
354 a half proportion being Protozoa.
355 In our sample, there are three abundant ASVs of Alveolata protists that represent
356 nearly 70% of the ITS region (Suppl. Fig. 1B, Forward-Only ITS database) in all
357 sequenced sites (S1-S4, S6, S7). Two of the three ASVs are Ciliophora (i.e. ciliates),
358 which is the most diverse phylum of protists, with 3,500 described species, most of
359 which are cosmopolites (Gao et al., 2016). It will therefore be interesting to analyze
360 more molecular markers in the future to distinguish the protist lineages, as well as to
361 microscopically study the protists to reach a closer taxonomic identification. Other

362 Protozoa ASVs were observed at low numbers and belong to the Amoebozoa
363 phylum, and the ancestral algae from the kingdom Chromista were also observed at
364 a low abundance (Suppl. Fig. 1B).
365 Although research on halophilic protozoan is still young, it has made great progress
366 in recent years (Harding & Simpson, 2018). Protozoa in general are grazing
367 organisms, as is the case with *Fabrea salina* ,one of the few classified low
368 abundance ITS ASVs in our study (Merge database, Suppl. Table 2). This ciliate is
369 present in microbial mats and feeds on *Cyanotece sp.*, a Cyanobacteria associated
370 with algae mats (Carrasco & Perissinotto, 2012). Indeed, in hypersaline
371 environments, most ciliates are known to be important components of the pelagic
372 microbial food loop (Liu et al., 2016). Amoebae have also been observed as grazers
373 (Hauer et al., 2001; Hauer & Rogerson, 2005; F. Post et al., 1983) on cyanobacteria
374 in surface mud samples from a salt pond in Eilat, within the Salton sea in Southern
375 California (Hauer & Rogerson, 2005). Even though the diversity of protists is low,
376 their prevalence, along with the large amount of viruses found in metagenomic
377 samples (28% of the metagenomes from Medina-Chávez et al., 2020), strongly
378 suggests that predator-prey interactions could be very important for the dynamics of
379 the system (Carreira et al., 2020).
380
381 ***Alpha and beta diversity***
382 The studied microbial mats –which are subject to extreme and fluctuating
383 environmental conditions– have a similar Shannon diversity as soil bacterial
384 communities (Dang et al., 2019; Wang et al., 2018). The Shannon Index accounts
385 for both species evenness and abundance; hence, it could sub-represent diversity if
386 most of the diversity is part of the rare biosphere. For example, Site 3 for the Eukarya
387 database had the highest Shannon value, despite having the lowest ASV number
388 (Table 1), due to its higher evenness distribution of taxa. Meanwhile, Chao1 only
389 compares the observed diversity with the expected, given a species distribution,
390 which more accurately reflects the total diversity of the site (Table 1; Suppl. Fig. 2A
391 and 2B).

392 Given the extraordinary patchiness of the observed diversity, exemplified by genera
393 composition differences between sample sites (Fig 2A), as well as unique
394 metabolomic patterns in each sample (Suppl. Fig. 4A&B), beta diversity analysis
395 showed a large turnover between sites despite the small scale (Suppl. Fig. 3).
396 Accordingly, the different domains analyzed (i.e., the Bacteria database or the
397 Eukarya database) had a distinctive association pattern, showing a statistically
398 significant geographic association only for the bacterial database.
399 Our results suggest a small taxonomical and functional core in these hyper-diverse
400 10 samples of the Archaean Domes, formed by bacterial and Eukaya ASVs shared
401 among all sites, that make up a low fraction of the total taxa, but are highly abundant
402 (183 16S rRNA ASVs, that comprises 3% of taxa (Fig. 3A) and 72.4% abundance of
403 all reads; 56 (6%) shared ITS ASVs with 94.7% abundance of all reads) (Fig. 3B).
404
405 ***Interactions in the Archaean Domes, inferred from the co-occurrence or co***
406 ***absence between sites.***
407 In this study, we performed a Pearson correlation analysis (Fig. 5) to identify
408 potential ecological roles and interactions between the most abundant ASVs within
409 the three databases and 22 archaeal ASVs. Negative correlations (i.e. absence or
410 lower than expected co-occurrence) can be used to identify metabolic competition,
411 separated niches, antagonistic interactions, or any other relationship precluding co-
412 occurrence (Saghaï et al., 2017). Meanwhile, positive correlations (i.e. co-occurr
413 frequently or always observed) encompass a variety of relationships that include
414 mutualism, symbiosis, parasitism, predation, common abiotic niche requirements
415 (which are particularly relevant to complex microbial mat communities), associations
416 with redox gradients, and metabolic syntrophy (Saghaï et al., 2017). We found more
417 positive correlations than negative (Suppl. Tab. 3) in our analysis. However, these
418 correlations do not necessarily indicate direct interactions, since two taxa that are
419 co-present may not be in direct physical or metabolic contact, due to the spatial
420 heterogeneity intrinsic to microbial mats. Therefore, this result should be taken
421 cautiously, given the Pearson correlation assumptions, as well as the consideration
422 that only a small (but abundant) fraction of the diversity is taken into account.

423 On the other hand, some of the twenty-two archaeal ASVs analyzed (Fig. 5) formed
424 a pattern of co-presence associations, which is worth noting since the same ASVs
425 were also part of the Archaea core observed in a time series metagenomic study
426 (Medina-Chávez et al., 2020). These positive associations reflect the presence of
427 taxa within samples: for example *Halorubrum*, *Halobacteria* and Wosearchaes are
428 positively associated because they were detected (i.e. coexist) in sample 2, and
429 *Halovivax*, *Haolorusis* and *Halorubraceae* were detected in sample 6; a similar
430 situation occurs for the fungi and Eukarya ASVs associated with them. Future
431 detailed studies, including metagenomic analyses, are required to understand the
432 mechanism of this potential cooperation, since co-cultivation techniques are difficult
433 given the differential life strategies of Archaea, which grow very slowly compared
434 with the faster growth of Fungi in culture.
435 It is interesting that, while most of the known fungal species are cosmopolitan and
436 generalists, a few others are specialists, usually adapted to extreme conditions
437 (Cantrell et al., 2011). For instance, Rozellomycota is a relatively large and
438 widespread group of eukaryotes, branching at the base of the fungal tree of life
439 (Corsaro et al., 2014). This group of fungi includes a number of amoebae parasites
440 that have developed unique morphological and genomic adaptations to intracellular
441 parasitism (Vávra & Lukeš, 2013). Thus, the utmost negative correlations observed
442 in two Rozellomycota ASVs (Fig. 5) might suggest the endoparasitic lifestyle of
443 these early-diverging fungi in the analyzed Archaean Domes.
444 The majority of the negative associations found among the abundant taxa of this
445 study were bacterial interactions (Fig. 5; Suppl. Table 3). Among them, bacteria-
446 bacteria negative interactions were mainly between different phyla. These
447 interactions are likely not based on metabolic competition, as they are mainly found
448 between different phyla that could not be sharing a niche. However, antagonism has
449 been reported previously in Cuatro Ciénegas bacterial taxa (Aguirre-von-Wobeser
450 et al., 2014; Moreno Fontalba, 2017; Pérez-Gutiérrez et al., 2013) and within cross-
451 kingdom interactions (Velez et al., 2018), which may account for the negative
452 correlations observed here. Nevertheless, it is important to remember that these are

453 only negative correlations, and experimental data is needed to demonstrate
454 antagonism in this system.
455
456 ***Phylogenetic diversity***
457 *Rare taxa*
458 A third of the abundance of the bacterial genera detected in our samples belongs to
459 rare bacterial taxa (Fig. 2A). The rare biosphere was more phylogenetically diverse
460 (Faith Pylogenetic Diversity index, Table 1) and phylogenetically disperse
461 (Phylogenetic Species Clustering, Fig. 4) than the abundant taxa within these
462 samples for both the 16S rRNA and ITS libraries, suggesting that environmental
463 filtering is not occurring for the rare biosphere in this site. This evidence suggests
464 that these rare taxa could be a large reservoir of genetic diversity, as well as a matrix
465 of rich microbial interactions and diverse metabolic functions within this microbial
466 mat (Jia et al., 2018), perhaps presenting collective adaptations to the extreme
467 conditions.
468
469 *Abundant taxa*
470 The pattern of phylogenetic clustering of the abundant ASVs is supported by
471 Pearson analysis, with a higher number of positive associations in general (reflecting
472 co-presence of taxa) and negative bacterial-bacterial associations between different
473 phyla. This pattern could be similar to some soil bacterial communities that typically
474 show a coexistence of phylogenetically close relatives (Bryant et al., 2009; Horner-
475 Devine & Bohannan, 2006), which may be the product of abiotic filtering or
476 competitive exclusion (Goberna et al., 2014). Competitive exclusion seems to be a
477 likely explanation for the phylogenetic clustering observed for abundant bacterial and
478 eukaryotic ASVs, as proposed by Goberna et al. (2014), since the presence of
479 compounds with antimicrobial properties suggests high levels of competition among
480 those abundant microbes.
481
482
483

484 ***Metabolomic profile***

485 The dynamic and complex metabolomic profiles of the studied microbial mat was
486 consistent with the highly diverse microbial community observed in the metagenomic
487 analysis (Medina-Chávez et al., 2020) (Fig. 6 and Suppl. Fig. 4A&B).
488 Even though the expression of regulatory genes responsible for secondary
489 metabolites production depends on several factors (e.g. nitrogen or phosphate
490 starvation, stressors like heat, pH and damage to the cell wall, among others) (Baral
491 et al., 2018), along with the lack of soil metabolomics studies and the solubility of the
492 compounds for LCMS analysis, we were still able to tentatively annotate several
493 classes of compounds with interesting biological properties (Fig. 7). Many of these
494 compounds were found to overlap between most of the samples: the antibiotics
495 indolactam 1 (Irie et al., 1990), 8,9-dihydroindanomycin (Li et al., 2009),
496 neoindanomycin (Rommel et al., 2011) described from *Streptomyces* species, and
497 martensine A reported from the marine red alga *Martensia fragilis* (Kirkup & Moore,
498 1983); the cytotoxic daryamide C (Asolkar et al., 2006), gibbestatin B (Kinashi &
499 Sakaguchi, 1984) and furaquinocin H (Ishibashi et al., 1991), from *Streptomyces*
500 strains; the germination inhibitor colletofragarone A1, from fungi *Colletotrichum*
501 *fragariae* and *C. capsiciae* (Inoue et al., 1996); benzastatin A (Kim et al., 1996) and
502 periconiasin G (Zaghouani et al., 2016) from *S. nitrosporeus* and *Periconia* sp. F-31
503 with free radical scavenger and weak anti-HIV activities; and phomamide and
504 tomaymycin I form *Phoma lingam* (Ferezou et al., 1980) and *Nocardia* sp. (Tozuka
505 et al., 1983) with no biological activity described. Other metabolites of interest were
506 found in specific samples, for example the antifungal agents griseofulvin and
507 dechlorogriseofulvin, produced by microorganisms of the genera *Penicillium*,
508 *Aspergillus*, *Xylaria*, *Coriolus*, *Palicourea*, *Memnoniella*, *Khauskia*, *Carpenteles*,
509 *Arthrinium*, *Nigrospora*, *Stachybotrys*, and *Streptomyces* (Atta-ur-Rahmanro, 2005;
510 Kimura et al., 1992; Knowles et al., 2019; Park et al., 2006) were identified only in
511 S7; the antimitotic agent nostodione A from the blue-green alga *Nostoc commune*
512 (Kobayashi et al., 1994) commune in samples S2 and S6-S8; and the mycotoxins
513 citreohybridone B (Kosemura, 2003), setosusin (Fujimoto et al., 1996), roridin E
514 (Böhner et al., 1965) and ganoboninone A (Ma et al., 2015) in samples S8-S10.

515 Interestingly, several observed ions (Suppl. Table 4) do not match with any data
516 reported and could represent potentially new secondary metabolites.
517 Several compounds associated with fungi and osmotrophs, as well as to other
518 Eukarya, reflect the importance of studying the potential role of microorganisms
519 besides bacteria, within microbial mats (Carreira et al., 2020).
520
521 **Perspectives**
522 In view of our results, the complex metabolomic data suggests local adaptive
523 processes, following eco-evolutionary dynamics. These dynamics would create
524 cohesive, diverse and fluctuating communities where taxa constantly and actively
525 modify their own ecological niche and that of others (niche construction) (Laland et
526 al., 2016; Odling-Smee et al., 2003, Van Der Hooft et al., 2020). However, this should
527 be tested in future studies, exploring the possibility that the rare biosphere could
528 fulfill the majority of the trophic levels and metabolic tasks, implementing
529 metabolomics, mesocosms, and metagenomic time series approaches. Additional
530 perspectives could evaluate the effect of environmental filtering, deepening the
531 analysis of the biotic interactions, including the rare biosphere.
532 The high phylogenetic diversity and phylogenetic dispersion of the rare biosphere
533 may suggest that there is a diverse “seed bank” in the aquifer of CCB, a deep
534 biosphere fed by magmatic energy (Wolaver 2013) that constantly “seeds” the
535 Archaean Domes community, along with deep water and particular minerals.
536 Therefore, in this scenario, eco-evolutionary feedbacks could enhance community
537 cohesion in Red Queen-like dynamics (Haafke et al., 2016), a hypothesis stating that
538 “biotic factors provide the basis for a self-driving perpetual motion of the effective
539 environment and so of the evolution of species affected by it” (Van Valen, 1973). In
540 our system, there may be a constant change in biotic interactions, as well as
541 evolutionary landscapes, while the abiotic variables (i.e., gases, nutrients, pH, salts)
542 are also constantly changing, as a product of community feedback within the deep
543 aquifer. In the Archaean Domes, active niche construction may have allowed the
544 communities to co-evolve around a stable species core, given an influx of new
545 neighbors of microbes and viruses (Taboada et al., 2018) from the deep biosphere,

546 which constantly assembles complex and new interactions. These ideas require
547 further testing, along with the community's resilience to fluctuations within these
548 extreme conditions.
549
550 **Methods**
551 *Sampling site and sample collection*
552 During the dry season (i. e. most of the year at CCB; Montiel-González et al., 2017),
553 the microbial mats of the Archaean domes remain humid and active under a salty
554 crust, which is then dissolved during the rainy season, allowing for increased
555 photosynthetic activity and the development of the dome-like structures.
556 The microbial mats of the Archaean domes were sampled during the rainy season
557 of 2018 (October), with ten evenly spaced samples (S1-S10) along a 1.5-meter
558 transect (26º 49' 41.7" N 102º 01' 28.7" W) in the 'Pozas Azules' ranch of Pronatura
559 Noroeste within CCB (Fig. 1). The salinity and pH were constant along the 1.5-meter
560 transect (salinity 53%, pH 9.8), and the average nutrient content showed a slight
561 stoichiometric imbalance (C:N:P 122:42:1), similar to the one measured during the
562 rainy season of 2016 (Medina-Chávez et al., 2020). Microbial mats and associated
563 sediments (8 cm) were collected and transferred to sterile conical tubes (50 mL),
564 stored at 4ºC, and subsequently frozen in liquid nitrogen until processing in the
565 laboratory.
566
567 *Total DNA extraction and amplicons sequencing*
568 Prior to DNA extraction, approximately 0.5 g of each sample was rinsed with sterile
569 water. Total DNA extraction was performed following the protocol reported in de
570 Anda et al. (2018), which is based on slight modifications from the Purdy et al. (1996)
571 protocol.
572 DNA was sequenced at the Laboratorio de Servicios Genómicos, LANGEBIO for the
573 V3-V4 region of the 16S rRNA gene (357F primer (Rudi et al., 1997), and the ITS
574 nDNA region (ITS1F/ITS4R for ITS; (White et al., 1990). For each sample**,** 5 mg of
575 genomic DNA (DO 260/280 1.8) was used; 16S amplicons were sequenced within
576 Illumina Next-Seq 500 platform (150 SE), and the ITS amplicons were sequenced

577 with a Mi-Seq platform (2x300 PE). All raw sequences generated are available at
578 GeneBank Bioproject PRJNA705156 (ITS accession SAMN18070760; 16S
579 accession SAMN18070761.
580
581 *Bioinformatics analyses*
582 The 16S rRNA amplicon reads were quality filtered and dereplicated using the QIIME
583 2 bioinformatics platform version 2019.7 (Bolyen et al., 2018). Sequences were
584 demultiplexed and truncated at the 20th bp from the left, and the 120th bp from the
585 right. Divisive Amplicon Denoising Algorithm 2 (dada2) was then used to filter by
586 sequence quality, remove chimeras, denoise, and create a table of amplicon
587 sequence variants (ASV) per sample. ASVs were then taxonomically classified using
588 the silva_132_99_v3v4_q2_2019-7 database. For all subsequent analyses the final
589 ASV table was rarefied to 760,000 reads. For abundant ASVs (>1%) and
590 Archaeobacteria ASVs, an additional taxonomic classification was conducted by
591 selecting those taxa with coincident classification across the results of *blastN* (both
592 type strain and 16S blast) (Altschul et al., 1990), the RDBP classifier (Q. Wang et
593 al., 2007), and Qiime2 (Silva database) (Bolyen et al., 2018; Quast et al., 2013).
594 The ITS amplicon reads were processed using the ITS-specific workflow of the
595 *dada2* v1.13.1 package (Callahan et al., 2016) in R (R Core Team, 2020). Briefly,
596 *cutadapt* was used to remove primer and adapter contamination from the raw reads
597 (Martin, 2011). Prior to determining ASVs, reads with inconsistent bases were
598 excluded, and reads were required to have less than two expected errors based on
599 their quality scores. ASVs classification was inferred from forward and reverse reads
600 using the run-specific error rates (Qiime2 and R code is available at
601 https://gitlab.com/lauasuar/archaean-domes-repository).
602 Due to the wide range of sizes of the ITS amplicons reported for fungal species in
603 CCB (485-782 bp; (Velez et al., 2016)), two different strategies were implemented
604 to define taxonomic diversity. First, the pre-denoised ASVs were merged after
605 excluding reads with an overlap of less than 12bp and reads with mismatches in the
606 overlapping region. Chimeras were removed using the consensus method of
607 "removeBimeraDenovo" implemented in dada2. The taxonomic assignment was

608 performed with the UNITE database (Nilsson et al., 2019), using the RDP naive
609 Bayesian classifier (Wang et al., 2007) available in the *dada2* package with a
610 minimum bootstrap value of 80. ASVs with a minimum of 85% identity and with E-
611 values lower than e-45 were retained (Merge ITS database, Suppl Table 1). ASVs
612 without taxonomic assignment (mostly non-fungi organisms) were classified using
613 *blastn*, where only those ASVs within identities greater than 90% were enlisted
614 (Suppl. Table 1). The remaining ASVs were considered non-classified.
615 As a great proportion of the reads failed to merge (~56%), a parallel classification
616 was implemented using the forward independently. The RDP naive Bayesian
617 classifier was used on the two sets of reads (forward and reverse) to check for
618 congruence in the classification between of ASVs. ASVs that had an assignment
619 bootstrap value lower than 50, or showed inconsistent classifications among forward
620 and reverse reads, were aligned to the NCBI database to corroborate their
621 taxonomic assignment. Even though some ASVs reached a genus level assignment,
622 the taxonomic classification of forward reads was limited to the phylum level (ITS
623 table, Suppl. Table 2); a more robust classification of ASVs was reached when using
624 forward ASVs, thus all subsequent analyses were performed using the forward-only
625 ASVs. The Eukaryotic classification followed the UNITE database. The ITS table
626 abundance was rarefied to 167,660 reads using the *vegan* package (Oksanen et al.,
627 2013) in R (R Core Team, 2020).
628 In sum, the 16S rRNA amplicon filtered database included 760,326–1,973,982 high
629 quality reads per sample, with a total of 6,063 ASVs. The ITS amplicon filtered
630 database included 167,660–352,720 high quality reads per sample, with a total of
631 923 ASVs. ITS amplicons were obtained for only six samples (S1, S2, S3, S4, S6
632 and S7) due to DNA depletion in four samples (S5, S8, S9 and S10). The ASV
633 abundance tables and the amplicons sequences are available at
634 https://gitlab.com/lauasuar/archaean-domes-repository.
635
636
637
638

639 *Alpha and beta diversity estimates*

640 To evaluate all samples from 16S (S1-S10) and 6 samples (S1-S4, S6, S7) from the
641 Forward-Only ITS database, we generated rarefied diversity plots using the *vegan*
642 package (Oksanen et al., 2013) in R (R Core Team 2020).

643 In order to visualize and count the number of overlapping ASVs within the ten
644 samples from the 16S rRNA gene and the six samples from the ITS region, we
645 constructed an UpSet plot using the *UpSetR* package (Conway et al., 2017) in R (R
646 Core Team 2020).

647 Alpha (i.e., Chao1, Shannon) and beta (i.e., Bray-Curtis, Jaccard) indices were
648 estimated using the 16S rRNA ASV abundance table, as implemented in Qiime2.
649 For the ITS ASV abundance table, alpha and beta diversity indices were estimated
650 with the the *phyloseq* package (McMurdie & Holmes, 2013) in R (R Core Team,
651 2020). The beta diversity indices were used to construct an UPGMA dendrogram of
652 samples (Carteron et al., 2012). Mantel tests (999 permutations) (Legendre &
653 Legendre, 2012) were conducted with the *vegan* package (Oksanen et al., 2013) to
654 unveil the relationships between beta diversity and geographic distance, as well as
655 between beta diversity and the metabolomic profile distance matrix (see below).

656

657 *Phylogenetic diversity*

658 We estimated phylogenetic diversity within samples using Faith's Phylogenetic
659 Diversity index (Faith, 1992) and the Phylogenetic Species Clustering index (Helmus
660 et al., 2007) using the *picante* package (Kembel et al., 2010) in R (R Core Team
661 2020). Given a phylogenetic tree, phylogenetic diversity (PD) estimates the total
662 length of branches encompassing a subset of taxa (*e.g.*, sampled communities),
663 where PD increases as the subset of taxa is more phylogenetically diverse (Faith,
664 1992). Phylogenetic Species Clustering (PSC) is a measure of the degree of
665 clustering of taxa across the phylogeny (Helmus et al., 2007), where a PSC value
666 approaching zero indicates that the subset of taxa are clustered within the
667 phylogeny.

668 To estimate the two metrics, we used the rarified diversity matrices and the
669 corresponding phylogenetic trees for bacterial and fungal ASVs, separately. We

670 tested the observed patterns of PSC across samples against 1,000 replicates under
671 a null model and estimated standardized effect sizes (SES) for this index. This
672 allowed us to identify samples that had more or less phylogenetic clustering than
673 expected by chance alone. To construct the null model, we randomized the entries
674 of the rarified diversity matrices while keeping total sample diversity constant. In
675 addition, we estimated PD and PSC for the most abundant and rare ASVs within
676 each site. To define rare and abundant ASVs, we estimated the first and third
677 quartiles (1Q, 3Q) of the distribution of ASV abundances for each site separately.
678 We used the sites' 1Q and 3Q as the thresholds to define rare and abundant ASVs;
679 the sites' 1Qs ranged from 3 to 16 reads per ASV, whereas the 3Qs ranged from 37
680 to 306 reads per ASV. We estimated SES for PD and PSC as defined above, using
681 matrices for rare and abundant ASV (R code for all phylogenetic diversity analysis
682 is available at https://gitlab.com/lauasuar/archaean-domes-repository).
683 The phylogenetic tree was generated by QIIME 2 (Bolyen et al., 2018) for 16S data.
684 For the ITS data (Forward-Only database), a phylogeny was obtained by applying
685 an equivalent phylogenetic QIIME 2 methodology, using Maftt (Katoh & Toh, 2010)
686 and FastTree (Price et al., 2009) within Cipres Science Gateway (Miller et al., 2010).
687
688 *Pearson correlation estimate among abundant taxa*
689 We carried out an analysis of correlated presences and absences of microbial taxa
690 across communities to identify plausible interactions and ecological roles within
691 microbial genera (Karpinets et al., 2018). To do this, we used a normalized
692 abundance of six-sites matrix that included ASVs from both ITS databases and 16S
693 rRNA gene library (Suppl Table 1): <1% abundance classified the ASV 16S
694 database, 22 six-sites archaea ASVs, and <1% classified the ASV ITS database
695 (calculated without the first three high abundance ASVs). Data was Hellinger
696 transformed, with the *vegan* package (Oksanen et al., 2013) in R (R Core Team,
697 2020). This normalized matrix was used to calculate the correlogram with Pearson
698 correlation (positive and negative strong correlation ($r \geq 0.9$, $P \leq 0.05$)) using the R
699 Stats v3.6.1 library (R Core Team, 2020) and *corrplot* package for the graph (Taiyun
700 & Viliam, 2017).

701 *Metabolomics*

702 *Soluble compounds extraction and LC-MS/MS analysis*

703 The samples (10 g each) were extracted with 60 mL of $CHCl_3$-MeOH (1:1) in an
704 orbital shaker at 150 rpm for 24 hrs. The mixture was filtered, and the solvent was
705 evaporated under reduced pressure. The dried extracts were reconstituted in 60 mL
706 of CH_3CN-MeOH (1:1) and defatted with hexanes. Then the CH_3CN-MeOH layer
707 was dried under a vacuum and resuspended in MeOH (LC-MS grade) to yield a
708 concentration of 1 mg mL^{-1}. All samples were filtered with a 0.22 μm membrane and
709 analyzed using a Waters Acquity Ultraperformance Liquid Chromatography (UPLC)
710 system (Waters Corp.) coupled to a Thermo Q Exactive Plus (ThermoFisher) mass
711 spectrometer. The UPLC separations were performed using an Acquity BEH C_{18}
712 column (50 mm × 2.1 mm I.D., 1.7 μm; Waters) equilibrated at 40 °C and a flow rate
713 set at 0.3 mL min^{-1}. The mobile phase consisted of a linear CH_3CN-H_2O (acidified
714 with 0.1% formic acid) gradient starting at 15% to 100% of CH_3CN over 8 min. The
715 mobile phase was held for another 1.5 min at 100% CH_3CN before returning to the
716 starting conditions. High-resolution mass spectrometry (HRMS) data and MS/MS
717 spectra were collected in the positive/negative switching electrospray ionization
718 (ESI) mode at a full scan range of *m/z* 150−2000, with the following settings: capillary
719 voltage, 5 V; capillary temperature, 300°C; tube lens offset, 35 V; spray voltage 3.80
720 kV; sheath gas flow and auxiliary gas flow, 35 and 20 arbitrary units, respectively.

721

722 *Untargeted metabolomics*

723 The HRMS-MS/MS raw data was individually aligned and filtered with MZmine 2.17
724 software (http://mzmine.sourceforge.net/) (Pluskal et al., 2010). Peak detection was
725 achieved as follows: *m/z* values were detected within each spectrum above a
726 baseline, a chromatogram was constructed for each of the *m/z* values that spanned
727 longer than 0.1 min, and finally, deconvolution algorithms were applied to each
728 chromatogram to recognize the individual chromatographic peaks. The parameters
729 were set as follows for peak detection: noise level (absolute value) at 1×10^6,
730 minimum peak duration 0.5 s, tolerance for *m/z* variation 0.05, and tolerance for *m/z*
731 intensity variation 20%. Deisotoping, peak list filtering, and retention time alignment

algorithm packages were employed to refine peak detection. The join align algorithm compiled a peak table according to the following parameters: the balance between *m/z* and retention time was set at 10.0 each, *m/z* tolerance at 0.05, and retention time tolerance size was defined as 2 min. The spectral data matrix (comprised of *m/z*, retention time, and peak area for each peak) was imported to Excel (Microsoft) for heatmap analysis using *R* (R Core Team, 2020).

Molecular networking was performed from the mzML files using the standard Global Natural Products Social (GNPS) molecular networking platform workflow with the spectral clustering algorithm (http://gnps.ucsd.edu; Aron et al, 2020). For spectral networks, parent mass of 0.01 Da and fragment ion tolerance of 0.02 Da were considered. For edges construction, a cosine score over 0.70 was fitted with a minimum of 4 matched peaks, and two nodes at least in the top 10 cosine scores (K) and maximum of 100 connected the components. After that, the network spectra were searched against GNPS spectral libraries (full data, feature-based molecular networking can be accessed here: https://gnps.ucsd.edu/ProteoSAFe/status.jsp?task=547303b749f041bb88eee71145de5184) and graphic visualization of molecular networking was performed in Cytoscape 3.8.0 (Shannon et al., 2003). The chemical profiles were also dereplicated using UV-absorption maxima and HRMS-MS/MS data against the Dictionary of Natural Products v 29.1 and Dictionary of Marine Natural Products 2019 (Taylor and Francis Group), MarinLite (University of Canterbury, New Zealand) and SciFinder (CAS) databases as described by El-Elimat et al. (El-Elimat et al., 2013), for fungal and bacterial small molecules. For candidate search, exact mass accuracy was set to 5 ppm. Heatmap visualization of metabolomic data table was generated in MataboAnalyst (Pang et al., 2020).

Acknowledgements

We would like to thank Dr. Erika Aguirre-Planter and Jessica Abril Hernández for technical and field assistance. We also thank PRONATURA Noreste for the access to the Pozas Azules ranch, and to Felipe García Oliva (CIEco, Biogeoquímica de suelos) for nutrient analysis of the samples. This research was supported by funding

from Sep-Ciencia Básica Conacyt grant 238245, and PAPIIT AG200319 / RG200319 and IN222220. The sampling was conducted with the collection permit SGPA/DGVS/03188/20 issued by Subsecretaría de Gestión para la protección Ambiental, Dirección General de Vida Silvestre.

Competing interests

The authors declare that no competing interests exist.

References

Aguirre-von-Wobeser, E., Soberón-Chávez, G., Eguiarte, L. E., Ponce-Soto, G. Y., Vázquez-Rosas-Landa, M., & Souza, V. (2014). Two-role model of an interaction network of free-living γ-proteobacteria from an oligotrophic environment. *Environmental Microbiology*, *16*(5), 1366–1377. https://doi.org/10.1111/1462-2920.12305

Altschul, S. F., Gish, W., Miller, W., Myers, E. W., & Lipman, D. J. (1990). Basic local alignment search tool. *Journal of Molecular Biology*, *215*(3), 403–410. https://doi.org/10.1016/S0022-2836(05)80360-2

Asolkar, R. N., Jensen, P. R., Kauffman, C. A., & Fenical, W. (2006). Daryamides A−C, Weakly Cytotoxic Polyketides from a Marine-Derived Actinomycete of the Genus Streptomyces Strain CNQ-085. *Journal of Natural Products*, *69*(12), 1756–1759. https://doi.org/10.1021/np0603828

Atta-ur-Rahmanro. (2005). Foreword. In B. T.-S. in N. P. C. Atta-ur-Rahman (Ed.), *Bioactive Natural Products (Part L)* (Vol. 32). Elsevier. https://doi.org/https://doi.org/10.1016/S1572-5995(05)80050-X

Baral, B., Akhgari, A., & Metsä-Ketelä, M. (2018). Activation of microbial secondary metabolic pathways: Avenues and challenges. *Synthetic and Systems Biotechnology*, *3*(3), 163–178. https://doi.org/https://doi.org/10.1016/j.synbio.2018.09.001

Bebout, B., Carpenter, S., Des Marais, D., Discipulo, M., Embaye, T., Garcia-Pichel, F., Hoehler, T., Hogan, M., Jahnke, L., Keller, R., Miller, S., Prufert-Bebout, L., Raleigh, C., Rothrock, M., & Turk-Kubo, K. (2002). Long-Term Manipulations of Intact Microbial Mat Communities in a Greenhouse Collaboratory: Simulating Earth's Present and Past Field Environments. *Astrobiology*, *2*, 383–402. https://doi.org/10.1089/153110702762470491

Ben Hania, W., Joseph, M., Schumann, P., Bunk, B., Fiebig, A., Spröer, C., Klenk, H. P., Fardeau, M. L., & Spring, S. (2015). Complete genome sequence and description of Salinispira pacifica gen. Nov., sp. nov., a novel spirochaete isolated form a hypersaline microbial mat. *Standards in Genomic Sciences*, *10*(FEBRUARY2015). https://doi.org/10.1186/1944-3277-10-7

Böhner, B., Fetz, E., Härri, E., Sigg, H. P., Stoll, C., & Tamm, C. (1965). Über die Isolierung von Verrucarin H, Verrucarin J, Roridin D und Roridin E aus Myrothecium-Arten. Verrucarine und Roridine, 8. Mitteilung. *Helvetica Chimica*

Acta, *48*(5), 1079–1087. https://doi.org/https://doi.org/10.1002/hlca.19650480515

Bolhuis, H., Cretoiu, M. S., & Stal, L. J. (2014). Molecular ecology of microbial mats. In *FEMS Microbiology Ecology* (Vol. 90, Issue 2, pp. 335–350). Oxford University Press. https://doi.org/10.1111/1574-6941.12408

Bolyen, E., Rideout, J. R., Dillon, M. R., Bokulich, N. A., Abnet, C. C., Al-ghalith, G. A., Alexander, H., Alm, E. J., Arumugam, M., Asnicar, F., Bai, Y., Bisanz, J. E., Bittinger, K., Brejnrod, A., Brislawn, C. J., Brown, T., Callahan, B. J., Caraballo-rodríguez, A. M., Chase, J., … Caporaso, J. G. (2018). QIIME 2: Reproducible, interactive, scalable, and extensible microbiome data science. *PeerJ*. https://doi.org/10.7287/peerj.preprints.27295v2

Bonilla-Rosso, G., Peimbert, M., Alcaraz, L. D., Hernández, I., Eguiarte, L. E., Olmedo-Alvarez, G., & Souza, V. (2012). Comparative metagenomics of two microbial mats at Cuatro Ciénegas Basin II: community structure and composition in oligotrophic environments. *Astrobiology*, *12*(7), 659–673. https://doi.org/10.1089/ast.2011.0724

Breitbart, M, Hollander, D., Nitti, A., Van Mooy, B., Siefert, J., & Souza, V. (2010). Modern freshwater microbialites of Cuatro Ciénegas, México. I: metagenomic and stable isotopic analyses to assess microbial community structure and function. In *Astrobiology Science Conference*.

Breitbart, Mya, Hoare, A., Nitti, A., Siefert, J., Haynes, M., Dinsdale, E., Edwards, R., Souza, V., Rohwer, F., & Hollander, D. (2009). Metagenomic and stable isotopic analyses of modern freshwater microbialites in Cuatro Ciénegas, Mexico. *Environmental Microbiology*, *11*(1), 16–34. https://doi.org/10.1111/j.1462-2920.2008.01725.x

Bryant, J. A., Lamanna, C., Morlon, H., Kerkhoff, A. J., Enquist, B. J., & Green, J. L. (2009). Microbes on mountainsides: Contrasting elevational patterns of bacterial and plant diversity. In *In the Light of Evolution* (Vol. 2, pp. 127–148). National Academies Press. https://doi.org/10.17226/12501

Callahan, B. J., McMurdie, P. J., Rosen, M. J., Han, A. W., Johnson, A. J. A., & Holmes, S. P. (2016). DADA2: High-resolution sample inference from Illumina amplicon data. *Nature Methods*, *13*(7), 581–583. https://doi.org/10.1038/nmeth.3869

Cantrell, S. A., Dianese, J., Fell, J., Gunde-Cimerman, N., & Zalar, P. (2011). Unusual fungal niches. *Mycologia*, *103*(6), 1161–1174. https://doi.org/10.3852/11-108

Cantrell, S. A., Tkavc, R., Gunde-Cimerman, N., Zalar, P., Acevedo, M., & Báez-Félix, C. (2013). Fungal communities of young and mature hypersaline microbial mats. *Mycologia*, *105*(4), 827–836. https://doi.org/10.3852/12-288

Cantrell, S., & Duval-Pérez, L. (2013). Microbial mats: An ecological niche for fungi. In *Frontiers in Microbiology* (Vol. 4, Issue APR). Frontiers Research Foundation.

Cardoso, D. C., Cretoiu, M. S., Stal, L. J., & Bolhuis, H. (2019). Seasonal development of a coastal microbial mat. *Scientific Reports*, *9*(1). https://doi.org/10.1038/s41598-019-45490-8

Carrasco, N. K., & Perissinotto, R. (2012). Development of a halotolerant community in the St. Lucia Estuary (South Africa) during a hypersaline phase. *PLoS ONE*, *7*(1). https://doi.org/10.1371/journal.pone.0029927

Carreira, C., Lonborg, C., Kühl, M., Lillebo, A. I., Sandaa, R. A., Villanueva, L., & Cruz, S. (2020). Fungi and viruses as important players in microbial mats. *FEMS Microbiology Ecology*, *96*(11), 1–13. https://doi.org/10.1093/femsec/fiaa187

Carteron, A., Jeanmougin, M., Leprieur, F., & Spatharis, S. (2012). Assessing the efficiency of clustering algorithms and goodness-of-fit measures using phytoplankton field data. *Ecological Informatics*, *9*, 64–68. https://doi.org/10.1016/j.ecoinf.2012.03.008

Choi, E. J., Beatty, D. S., Paul, L. A., Fenical, W., & Jensen, P. R. (2013). Mooreia alkaloidigena gen. nov., sp. nov. and Catalinimonas alkaloidigena gen. nov., sp. nov., alkaloid-producing marine bacteria in the proposed families Mooreiaceae fam. nov. and Catalimonadaceae fam. nov. in the phylum Bacteroidetes. *International Journal of Systematic and Evolutionary Microbiology*, *63*(PART4), 1219–1228. https://doi.org/10.1099/ijs.0.043752-0

Conway, J. R., Lex, A., & Gehlenborg, N. (2017). UpSetR: An R package for the visualization of intersecting sets and their properties. *Bioinformatics*, *33*(18), 2938–2940. https://doi.org/10.1093/bioinformatics/btx364

Corsaro, D., Walochnik, J., Venditti, D., Steinmann, J., Müller, K.-D., & Michel, R. (2014). Microsporidia-like parasites of amoebae belong to the early fungal lineage Rozellomycota. *Parasitology Research*, *113*(5), 1909–1918. https://doi.org/10.1007/s00436-014-3838-4

Dang, Q., Tan, W., Zhao, X., Li, D., Li, Y., Yang, T., Li, R., Zu, G., & Xi, B. (2019). Linking the response of soil microbial community structure in soils to long-term wastewater irrigation and soil depth. *Science of the Total Environment*, *688*, 26–36. https://doi.org/10.1016/j.scitotenv.2019.06.138

De Anda, V., Zapata-Peñasco, I., Blaz, J., Poot-Hernández, A. C., Contreras-Moreira, B., González-Laffitte, M., Gámez-Tamariz, N., Hernández-Rosales, M., Eguiarte, L. E., & Souza, V. (2018). Understanding the mechanisms behind the response to environmental perturbation in microbial mats: A metagenomic-network based approach. *Frontiers in Microbiology*, *9*(NOV). https://doi.org/10.3389/fmicb.2018.02606

De Wit, R., Guerrero, M. C., Legaz, A., Jonkers, H. M., Blocier, L., Gumiaux, C., & Gautret, P. (2013). Conservation of a permanent hypersaline lake: Management options evaluated from decadal variability of coleofasciculus chthonoplastes microbial mats. *Aquatic Conservation: Marine and Freshwater Ecosystems*, *23*(4), 532–545. https://doi.org/10.1002/aqc.2319

Des Marais, D. (2010). *Marine Hypersaline Microcoleus-Dominated Cyanobacterial Mats in the Saltern at Guerrero Negro, Baja California Sur, Mexico: A System-Level Perspective* (Vol. 14, pp. 401–420). https://doi.org/10.1007/978-90-481-3799-2_21

Edgcomb, V. P., Bernhard, J. M., Summons, R. E., Orsi, W., Beaudoin, D., & Visscher, P. T. (2014). Active eukaryotes in microbialites from Highborne Cay, Bahamas, and Hamelin Pool (Shark Bay), Australia. *ISME Journal*, *8*(2), 418–429. https://doi.org/10.1038/ismej.2013.130

El-Elimat, T., Figueroa, M., Ehrmann, B. M., Cech, N. B., Pearce, C. J., & Oberlies, N. H. (2013). High-Resolution MS, MS/MS, and UV Database of Fungal Secondary Metabolites as a Dereplication Protocol for Bioactive Natural Products. *Journal of Natural Products*, *76*(9), 1709–1716.

https://doi.org/10.1021/np4004307
Elser, J. J., Schampel, J. H., Garcia-Pichel, F., Wade, B. D., Souza, V., Eguiarte, L., Escalante, A., & Farmer, J. D. (2005). Effects of phosphorus enrichment and grazing snails on modern stromatolitic microbial communities. *Freshwater Biology*, *50*(11), 1808–1825. https://doi.org/10.1111/j.1365-2427.2005.01451.x
Elser, J. J., Watts, J., Schampel, J. H., & Farmer, J. (2006). Early Cambrian food webs on a trophic knife-edge? A hypothesis and preliminary data from a modern stromatolite-based ecosystem. *Ecology Letters*, *9*(3), 292–300. https://doi.org/10.1111/j.1461-0248.2005.00873.x
Faith, D. P. (1992). Conservation evaluation and phylogenetic diversity. *Biological Conservation*, *61*(1), 1–10. https://doi.org/https://doi.org/10.1016/0006-3207(92)91201-3
Ferezou, J.-P., Quesneau-Thierry, A., Barbier, M., Kollmann, A., & Bousquet, J.-F. (1980). Structure and synthesis of phomamide, a new piperazine-2,5-dione related to the sirodesmins, isolated from the culture medium of Phoma lingam Tode. *Journal of the Chemical Society, Perkin Transactions 1*, *0*, 113–115. https://doi.org/10.1039/P19800000113
Fujimoto, H., Neghisi, E., Yamaguchi, K., Nishi, N., & Yamazaki, M. (1996). Isolation of New Tremorgenic Metabolites from an Ascomycete, Corynascus setosus. *Chemical & Pharmaceutical Bulletin*, *44*(10), 1843–1848. https://doi.org/10.1248/cpb.44.1843
Gerdes, G. (2010). What are microbial mats? *Microbial Mats: Modern and Ancient Microorganisms in Stratified Systems*, 3–25.
Gerdes, Gisela, Claes, M., Dunajtschik-Piewak, K., Riege, H., Krumbein, W. E., & Reineck, H.-E. (1993). Contribution of microbial mats to sedimentary surface structures. *Facies*, *29*(1), 61. https://doi.org/10.1007/BF02536918
Glassman, S. I., & Martiny, J. B. H. (2018). Broadscale Ecological Patterns Are Robust to Use of Exact. *MSphere*, *3*(4), e00148-18.
Goberna, M., Navarro-Cano, J. A., Valiente-Banuet, A., García, C., & Verdú, M. (2014). Abiotic stress tolerance and competition-related traits underlie phylogenetic clustering in soil bacterial communities. *Ecology Letters*, *17*(10), 1191–1201. https://doi.org/10.1111/ele.12341
Gutiérrez-Preciado, A., Saghaï, A., Moreira, D., Zivanovic, Y., Deschamps, P., & López-García, P. (2018). Functional shifts in microbial mats recapitulate early Earth metabolic transitions. *Nature Ecology and Evolution*, *2*(11), 1700–1708. https://doi.org/10.1038/s41559-018-0683-3
Haafke, J., Abou Chakra, M., & Becks, L. (2016). Eco-evolutionary feedback promotes Red Queen dynamics and selects for sex in predator populations. *Evolution*, *70*(3), 641–652. https://doi.org/https://doi.org/10.1111/evo.12885
Harding, T., & Simpson, A. G. B. (2018). Recent Advances in Halophilic Protozoa Research. In *Journal of Eukaryotic Microbiology* (Vol. 65, Issue 4, pp. 556–570). Blackwell Publishing Inc. https://doi.org/10.1111/jeu.12495
Hauer, G., & Rogerson, A. (2005). Heterotrophic Protozoa from Hypersaline Environments. In Gunde-Cimerman Nina, A. and Oren, & and P. Ana (Eds.), *Adaptation to Life at High Salt Concentrations in Archaea, Bacteria, and Eukarya* (pp. 519–539). Springer Netherlands.
Hauer, G., Rogerson, A., & Anderson, O. R. (2001). Platyamoeba pseudovannellida

n. sp., a naked amoeba with wide salt tolerance isolated from the Salton Sea, California. *Journal of Eukaryotic Microbiology*, *48*(6), 663–669. https://doi.org/10.1111/j.1550-7408.2001.tb00206.x

Helmus, M. R., Bland, T. J., Williams, C. K., & Ives, A. R. (2007). Phylogenetic measures of biodiversity. *The American Naturalist*, *169*(3). https://doi.org/10.1086/511334

Horner-Devine, M. C., & Bohannan, B. J. M. (2006). Phylogenetic clustering and overdispersion in bacterial communities. *Ecology*, *87*(7 SUPPL.).

Inoue, M., Takenaka, H., Tsurushima, T., Miyagawa, H., & Ueno, T. (1996). Colletofragarones A1 and A2, novel germination self-inhibitors from the fungus Colletotrichum fragariae. *Tetrahedron Letters*, *37*(32), 5731–5734. https://doi.org/https://doi.org/10.1016/0040-4039(96)01212-9

Irie, K., Kajiyama, S., Koshimizu, K., Hayashi, H., & Arai, M. (1990). Isolation and biosynthesis of (−)-indolactam I, a new congener of indole alkaloid tumor promoter teleocidins. *Tetrahedron Letters*, *31*(50), 7337–7340. https://doi.org/https://doi.org/10.1016/S0040-4039(00)88559-7

Ishibashi, M., Funayama, S., Anraku, Y., Komiyama, K., & Omtura, S. (1991). Novel antibiotics, furaquinocins C, D, E, F, G and H. *The Journal of Antibiotics*, *44*(4), 390–395. https://doi.org/10.7164/antibiotics.44.390

Jia, X., Dini-Andreote, F., & Falcão Salles, J. (2018). Community Assembly Processes of the Microbial Rare Biosphere. *Trends in Microbiology*, *26*(9), 738–747. https://doi.org/10.1016/j.tim.2018.02.011

Karpinets, T. V., Gopalakrishnan, V., Wargo, J., Futreal, A. P., Schadt, C. W., & Zhang, J. (2018). Linking associations of rare low-abundance species to their environments by association networks. *Frontiers in Microbiology*, *9*(MAR). https://doi.org/10.3389/fmicb.2018.00297

Katoh, K., & Toh, H. (2010). Parallelization of the MAFFT multiple sequence alignment program. *Bioinformatics*, *26*(15), 1899–1900. https://doi.org/10.1093/bioinformatics/btq224

Kembel, S., Cowan, P., Helmus, M., Cornwell, W., Morlon, H., Ackerly, D., Blomberg, S., & Webb, C. (2010). Picante: R tools for integrating phylogenies and ecology. *Bioinformatics*, *26*, 1463–1464.

Kim, W. G., Kim, J. P., & Yoo, I. D. (1996). Benzastatins A, B, C, and D : New free radical scavengers from Streptomyces nitrosporeus 30643 II. Structure determination. *Journal of Antibiotics*, *49*(1), 26–30. https://doi.org/10.7164/antibiotics.49.26

Kimura, Y., Shiojima, K., Nakajima, H., & Hamasaki, T. (1992). Structure and Biological Activity of Plant Growth Regulators Produced by Penicillium sp. No. 31f. *Bioscience, Biotechnology, and Biochemistry*, *56*(7), 1138–1139. https://doi.org/10.1271/bbb.56.1138

Kinashi, H., & Sakaguchi, K. (1984). Structures of Antibiotics 2-11-A and B. *Agricultural and Biological Chemistry*, *48*(1), 245–247. https://doi.org/10.1080/00021369.1984.10866129

Kirkup, M. P., & Moore, R. E. (1983). Indole alkaloids from the marine red alga Martensia fragilis. *Tetrahedron Letters*, *24*(20), 2087–2090. https://doi.org/https://doi.org/10.1016/S0040-4039(00)81851-1

Knowles, S. L., Raja, H. A., Wright, A. J., Lee, A. M. L., Caesar, L. K., Cech, N. B.,

Mead, M. E., Steenwyk, J. L., Ries, L. N. A., Goldman, G. H., Rokas, A., & Oberlies, N. H. (2019). Mapping the Fungal Battlefield: Using in situ Chemistry and Deletion Mutants to Monitor Interspecific Chemical Interactions Between Fungi. *Frontiers in Microbiology*, *10*, 285. https://doi.org/10.3389/fmicb.2019.00285

Kobayashi, A., Kaiiyama, S. ichiro, Inawaka, K., Kanzaki, H., & Kawazu, K. (1994). Nostodione A, a Novel Mitotic Spindle Poison* from a Blue-Green Alga Nostoc commune. *Zeitschrift Fur Naturforschung - Section C Journal of Biosciences*, *49*(7–8), 464–470. https://doi.org/10.1515/znc-1994-7-812

Kosemura, S. (2003). Meroterpenoids from Penicillium citreo-viride B. IFO 4692 and 6200 hybrid. *Tetrahedron*, *59*(27), 5055–5072. https://doi.org/https://doi.org/10.1016/S0040-4020(03)00739-7

Laland, K., Matthews, B., & Feldman, M. W. (2016). An introduction to niche construction theory. *Evolutionary Ecology*, *30*(2), 191–202. https://doi.org/10.1007/s10682-016-9821-z

Legendre, P., & Legendre, L. (2012). *Numerical Ecology* (3rd ed.). Elsevier, Amsterdam.

Li, C., Roege, K. E., & Kelly, W. L. (2009). Analysis of the Indanomycin Biosynthetic Gene Cluster from Streptomyces antibioticus NRRL 8167. *ChemBioChem*, *10*(6), 1064–1072. https://doi.org/https://doi.org/10.1002/cbic.200800822

Liang, R., Davidova, I. A., Marks, C. R., Stamps, B. W., Harriman, B. H., Stevenson, B. S., Duncan, K. E., & Suflita, J. M. (2016). Metabolic capability of a predominant Halanaerobium sp. in hydraulically fractured gas wells and its implication in pipeline corrosion. *Frontiers in Microbiology*, *7*(JUN). https://doi.org/10.3389/fmicb.2016.00988

Liu, J., Meng, Z., Liu, X., & Zhang, X. (2019). Microbial assembly, interaction, functioning, activity and diversification: a review derived from community compositional data. *Marine Life Science & Technology*, *1*(1), 112–128. https://doi.org/10.1007/s42995-019-00004-3

Liu, W., Xu, D., Ma, H., Al-Farraj, S. A., Warren, A., & Yi, Z. (2016). Taxonomy and molecular systematics of three oligotrich (s.l.) ciliates including descriptions of two new species, Strombidium guangdongense sp. nov. and Strombidinopsis sinicum sp. nov. (Protozoa, Ciliophora). *Systematics and Biodiversity*, *14*(5), 452–465. https://doi.org/10.1080/14772000.2016.1162872

Liu, X., Li, M., Castelle, C. J., Probst, A. J., Zhou, Z., Pan, J., Liu, Y., Banfield, J. F., & Gu, J. D. (2018). Insights into the ecology, evolution, and metabolism of the widespread Woesearchaeotal lineages. *Microbiome*, *6*(1), 1–16. https://doi.org/10.1186/s40168-018-0488-2

López-Lozano, N. E., Heidelberg, K. B., Nelson, W. C., García-Oliva, F., Eguiarte, L. E., & Souza, V. (2013). Microbial secondary succession in soil microcosms of a desert oasis in the Cuatro Cienegas Basin, Mexico. *PeerJ*, *1*, e47. https://doi.org/10.7717/peerj.47

Ma, K., Li, L., Bao, L., He, L., Sun, C., Zhou, B., Si, S., & Liu, H. (2015). Six new 3,4-seco-27-norlanostane triterpenes from the medicinal mushroom Ganoderma boninense and their antiplasmodial activity and agonistic activity to LXRβ. *Tetrahedron*, *71*(12), 1808–1814. https://doi.org/https://doi.org/10.1016/j.tet.2015.02.002

Margulis, L., Ashen, J. B., Sole, M., & Guerrero, R. (2006). Composite, large spirochetes from microbial mats: spirochete structure review. *Proceedings of the National Academy of Sciences*, *90*(15), 6966–6970. https://doi.org/10.1073/pnas.90.15.6966

Martin, M. (2011). Cutadapt removes adapter sequences from high-throughput sequencing reads. *EMBnet. Journal*, *17*(1), 10–12.

Mayfield, M. M., & Levine, J. M. (2010). Opposing effects of competitive exclusion on the phylogenetic structure of communities. *Ecology Letters*, *13*, 1085–1093. https://doi.org/https://doi.org/10.1111/j.1461-0248.2010.01509.x

McGonigle, J. M., Bernau, J. A., Bowen, B. B., & Brazelton, W. J. (2019). Robust Archaeal and Bacterial Communities Inhabit Shallow Subsurface Sediments of the Bonneville Salt Flats. *MSphere*, *4*(4), 1–12. https://doi.org/10.1128/msphere.00378-19

McMurdie, P. J., & Holmes, S. (2013). Phyloseq: An R Package for Reproducible Interactive Analysis and Graphics of Microbiome Census Data. *PLoS ONE*, *8*(4). https://doi.org/10.1371/journal.pone.0061217

Medina-Chávez, N. O., Viladomat-Jasso, M., Olmedo-Álvarez, G., Eguiarte Luis, E., Souza, V., & De la Torre-Zavala, S. (2019). Diversity of Archaea domain in Cuatro Cienegas Basin: Archean Domes. *Submitted*.

Miller, M. A., Pfeiffer, W., & Schwartz, T. (2010). Creating the CIPRES Science Gateway for inference of large phylogenetic trees. *2010 Gateway Computing Environments Workshop, GCE 2010*. https://doi.org/10.1109/GCE.2010.5676129

Moreno Fontalba, C. (2017). Ecología de las interacciones entre bacterias en Cuatro Ciénegas Coahuila México. *Instituto de Ecologia UNAM Master Thesis Https://Bit.Ly/2n0sdMp*.

Nilsson, R. H., Larsson, K. H., Taylor, A. F. S., Bengtsson-Palme, J., Jeppesen, T. S., Schigel, D., Kennedy, P., Picard, K., Glöckner, F. O., Tedersoo, L., Saar, I., Kõljalg, U., & Abarenkov, K. (2019). The UNITE database for molecular identification of fungi: Handling dark taxa and parallel taxonomic classifications. *Nucleic Acids Research*, *47*(D1), D259–D264. https://doi.org/10.1093/nar/gky1022

Nitti, A., Daniels, C. A., Siefert, J., Souza, V., Hollander, D., & Breitbart, M. (2012). Spatially Resolved Genomic, Stable Isotopic, and Lipid Analyses of a Modern Freshwater Microbialite from Cuatro Ciénegas, Mexico. *Astrobiology*, *12*(7), 685–698. https://doi.org/10.1089/ast.2011.0812

Nutman, A. P., Bennett, V. C., Friend, C. R. L., Van Kranendonk, M. J., & Chivas, A. R. (2016). Rapid emergence of life shown by discovery of 3,700-million-year-old microbial structures. *Nature*, *537*(7621), 535–538. https://doi.org/10.1038/nature19355

Odling-Smee, F. J., Laland, K. N., & Feldman, M. W. (2003). *The Neglected Process in Evolution (MPB-37)*. Princeton University Press. http://www.jstor.org/stable/j.ctt24hqpd

Oksanen, J., Blanchet, F. G., Kindt, R., Legendre, P., Minchin, P. R., O'Hara, R. B., Simpson, G. L., Solymos, P., Stevens, M. H. H., & Wagner, H. (2013). *Vegan: Community Ecology Package. R package version 2.0-8. http://CRAN.R-project.org/package=vegan. Accessed 2013 Nov* (R package version 2.0-8.).

http://cran.r-project.org/package=vegan

Ortiz-Alvarez, R., & Casamayor, E. O. (2016). High occurrence of Pacearchaeota and Woesearchaeota (Archaea superphylum DPANN) in the surface waters of oligotrophic high-altitude lakes. *Environmental Microbiology Reports*, *8*(2), 210–217. https://doi.org/10.1111/1758-2229.12370

Paerl Hans W.and Yannarell, A. C. (2010). Environmental Dynamics, Community Structure and Function in a Hypersaline Microbial Mat. In A. Seckbach Josephand Oren (Ed.), *Microbial Mats: Modern and Ancient Microorganisms in Stratified Systems* (pp. 421–442). Springer Netherlands. https://doi.org/10.1007/978-90-481-3799-2_22

Pajares, S., Bonilla-Rosso, G., Travisano, M., Eguiarte, L. E., & Souza, V. (2012). Mesocosms of aquatic bacterial communities from the Cuatro Cienegas Basin (Mexico): a tool to test bacterial community response to environmental stress. *Microbial Ecology*, *64*(2), 346–358. https://doi.org/10.1007/s00248-012-0045-7

Pajares, S., Eguiarte, L. E., Bonilla-Rosso, G., & Souza, V. (2013). Drastic changes in aquatic bacterial populations from the Cuatro Cienegas Basin (Mexico) in response to long-term environmental stress. *Antonie van Leeuwenhoek*, *104*(6), 1159–1175. https://doi.org/10.1007/s10482-013-0038-7

Pang, Z., Chong, J., Li, S., & Xia, J. (2020). Metaboanalystr 3.0: Toward an optimized workflow for global metabolomics. *Metabolites*, *10*(5). https://doi.org/10.3390/metabo10050186

Papineau, D. (2010). Global Biogeochemical Changes at Both Ends of the Proterozoic: Insights from Phosphorites. *Astrobiology*, *10*(2), 165–181. https://doi.org/10.1089/ast.2009.0360

Park, J. S., Cho, B. C., & Simpson, A. G. B. (2006). Halocafeteria seosinensis gen. et sp. nov. (Bicosoecida), a halophilic bacterivorous nanoflagellate isolated from a solar saltern. *Extremophiles*, *10*(6), 493–504. https://doi.org/10.1007/s00792-006-0001-x

Pasulka, A., Hu, S. K., Countway, P. D., Coyne, K. J., Cary, S. C., Heidelberg, K. B., & Caron, D. A. (2019). SSU-rRNA Gene Sequencing Survey of Benthic Microbial Eukaryotes from Guaymas Basin Hydrothermal Vent. *Journal of Eukaryotic Microbiology*. https://doi.org/10.1111/jeu.12711

Peimbert, M., Alcaraz, L. D., Bonilla-Rosso, G., Olmedo-Alvarez, G., García-Oliva, F., Segovia, L., Eguiarte, L. E., & Souza, V. (2012). Comparative metagenomics of two microbial mats at Cuatro Ciénegas Basin I: ancient lessons on how to cope with an environment under severe nutrient stress. *Astrobiology*, *12*(7), 648–658. https://doi.org/10.1089/ast.2011.0694

Pérez-Gutiérrez, R. A., López-Ramírez, V., Islas, Á., Alcaraz, L. D., Hernández-González, I., Olivera, B. C. L., Santillán, M., Eguiarte, L. E., Souza, V., Travisano, M., & Olmedo-Alvarez, G. (2013). Antagonism influences assembly of a Bacillus guild in a local community and is depicted as a food-chain network. *ISME Journal*, *7*(3), 487–497. https://doi.org/10.1038/ismej.2012.119

Planavsky, N. J., Rouxel, O. J., Bekker, A., Lalonde, S. V., Konhauser, K. O., Reinhard, C. T., & Lyons, T. W. (2010). The evolution of the marine phosphate reservoir. *Nature*, *467*(7319), 1088–1090. https://doi.org/10.1038/nature09485

Pluskal, T., Castillo, S., Villar-Briones, A., & Orešič, M. (2010). MZmine 2: Modular framework for processing, visualizing, and analyzing mass spectrometry-based

molecular profile data. *BMC Bioinformatics*, *11*. https://doi.org/10.1186/1471-2105-11-395

Post, D. M., & Palkovacs, E. P. (2009). Eco-evolutionary feedbacks in community and ecosystem ecology: Interactions between the ecological theatre and the evolutionary play. *Philosophical Transactions of the Royal Society B: Biological Sciences*, *364*(1523), 1629–1640. https://doi.org/10.1098/rstb.2009.0012

Post, F., Borowitzka, L., Borowitzka, M., Mackay, B., & Moulton, T. (1983). The protozoa of a Western Australian hypersaline lagoon. *Hydrobiologia*, *105*(1), 95–113. https://doi.org/10.1007/BF00025180

Price, M. N., Dehal, P. S., & Arkin, A. P. (2009). Fasttree: Computing large minimum evolution trees with profiles instead of a distance matrix. *Molecular Biology and Evolution*, *26*(7), 1641–1650. https://doi.org/10.1093/molbev/msp077

Prieto-Barajas, C. M., Valencia-Cantero, E., & Santoyo, G. (2018). Microbial mat ecosystems: Structure types, functional diversity, and biotechnological application. In *Electronic Journal of Biotechnology* (Vol. 31, pp. 48–56). Pontificia Universidad Catolica de Valparaiso. https://doi.org/10.1016/j.ejbt.2017.11.001

Purdy, K. J., Embley, T. M., Takii, S., & Nedwell, A. D. B. (1996). Rapid Extraction of DNA and rRNA from Sediments by a Novel Hydroxyapatite Spin-Column Method. In *APPLIED AND ENVIRONMENTAL MICROBIOLOGY* (Vol. 62, Issue 10).

Quast, C., Pruesse, E., Yilmaz, P., Gerken, J., Schweer, T., Yarza, P., Peplies, J., & Glöckner, F. O. (2013). The SILVA ribosomal RNA gene database project: improved data processing and web-based tools. *Nucleic Acids Research*, *41*(D1), D590–D596. https://doi.org/10.1093/nar/gks1219

R Core Team. (2020). *R: A language and environment for statistical computing. R Foundation for Statistical Computing, Vienna, Austria*. R Foundation for Statistical Computing. http://www.r-project.org/

Ramos, V. M. C., Castelo-Branco, R., Leão, P. N., Martins, J., Carvalhal-Gomes, S., da Silva, F. S., Filho, J. G. M., & Vasconcelos, V. M. (2017). Cyanobacterial diversity in microbial mats from the hypersaline lagoon system of Araruama, Brazil: An in-depth polyphasic study. *Frontiers in Microbiology*, *8*(JUN), 1–16. https://doi.org/10.3389/fmicb.2017.01233

Rebollar, E. A., Avitia, M., Eguiarte, L. E., González-González, A., Mora, L., Bonilla-Rosso, G., & Souza, V. (2012). Water-sediment niche differentiation in ancient marine lineages of Exiguobacterium endemic to the Cuatro Cienegas Basin. *Environmental Microbiology*, *14*(9), 2323–2333. https://doi.org/10.1111/j.1462-2920.2012.02784.x

Rommel, K. R., Li, C., & Kelly, W. L. (2011). Identification of a Tetraene-Containing Product of the Indanomycin Biosynthetic Pathway. *Organic Letters*, *13*(10), 2536–2539. https://doi.org/10.1021/ol200570u

Rudi, K., Skulberg, O. M., Larsen, F., & Jakobsen, K. S. (1997). Strain characterization and classification of oxyphotobacteria in clone cultures on the basis of 16S rRNA sequences from the variable regions V6, V7, and V8. *Applied and Environmental Microbiology*, *63*(7), 2593–2599.

Saghaï, A., Gutiérrez-Preciado, A., Deschamps, P., Moreira, D., Bertolino, P., Ragon, M., & López-García, P. (2017). Unveiling microbial interactions in

stratified mat communities from a warm saline shallow pond. *Environmental Microbiology*, *19*(6), 2405–2421. https://doi.org/10.1111/1462-2920.13754

Sardans, J., Peñuelas, J., & Rivas-Ubach, A. (2011). Ecological metabolomics: Overview of current developments and future challenges. *Chemoecology*, *21*(4), 191–225. https://doi.org/10.1007/s00049-011-0083-5

Souza, V., Eguiarte, L. E., Moreno-Letelier, A., Travisano, M., Alcaraz, L. D., & Olmedo, G. (2018). The lost world of Cuatro Ciénegas Basin, a relictual bacterial niche in a desert oasis. *ELife*, *7*. https://doi.org/10.7554/eLife.38278

Souza, V., Espinosa-Asuar, L., Escalante, A. E., Eguiarte, L. E., Farmer, J., Forney, L., Lloret, L., Rodriguez-Martinez, J. M., Soberon, X., Dirzo, R., Elser, J. J., Rodríguez-Martínez, J. M., Soberón, X., Dirzo, R., Elser, J. J., Forney, L., Sobero, X., & Elser, J. J. (2006). An endangered oasis of aquatic microbial biodiversity in the Chihuahuan desert. *Proceedings of the National Academy of Sciences of the United States of America*, *103*(17), 6565–6570. https://doi.org/10.1073/pnas.0601434103

Souza, V., Olmedo-Álvarez, G., & Eguiarte, L. E. (Eds.). (2018). *Cuatro Ciénegas Ecology, Natural History and Microbiology*. Springer International Publishing. https://doi.org/10.1007/978-3-319-93423-5

Souza, V., Siefert, J., Escalante, A. E., Elser, J. J., & Eguiarte, L. E. (2012). The Cuatro Ciénegas Basin in Coahuila, Mexico: an astrobiological Precambrian Park. *Astrobiology*, *12*(7), 641–647. https://doi.org/10.1089/ast.2011.0675

Stolz, J. F. (2000). Structure of Microbial Mats and Biofilms. In S. M. Riding Robert E.and Awramik (Ed.), *Microbial Sediments* (pp. 1–8). Springer Berlin Heidelberg. https://doi.org/10.1007/978-3-662-04036-2_1

Taboada, B., Isa, P., Gutiérrez-Escolano, A. L., M. del ángel, R., Ludert, J. E., Vázquez, N., Tapia-Palacios, M. A., Chávez, P., Garrido, E., Espinosa, A. C., Eguiarte, L. E., López, S., Souza, V., & Arias, C. F. (2018). The geographic structure of viruses in the Cuatro Ciénegas Basin, a unique oasis in northern Mexico, reveals a highly diverse population on a small geographic scale. *Applied and Environmental Microbiology*, *84*(11). https://doi.org/10.1128/AEM.00465-18

Taiyun, W., & Viliam, S. (2017). *R package "corrplot": Visualization of a Correlation Matrix (Version 0.84)*. https://github.com/taiyun/corrplot

Tozuka, Z., Takasugi, H., & Takaya, T. (1983). Studies on tomaymycin. II. Total syntheses of the antitumor antibiotics, E-and Z-tomaymycins. *The Journal of Antibiotics*, *36*(3), 276–282. https://doi.org/10.7164/antibiotics.36.276

Van Der Hooft, J. J. J., Mohimani, H., Bauermeister, A., Dorrestein, P. C., Duncan, K. R., & Medema, M. H. (2020). Linking genomics and metabolomics to chart specialized metabolic diversity. *Chemical Society Reviews*, *49*(11), 3297–3314. https://doi.org/10.1039/d0cs00162g

Van Valen, L. (1973). A new evolutionary law. *Evolutionary Theory* , *1*, 1–30.

Vávra, J., & Lukeš, J. (2013). Microsporidia and 'The Art of Living Together.' In *Advances in Parasitology* (Vol. 82, pp. 253–319). Academic Press. https://doi.org/10.1016/B978-0-12-407706-5.00004-6

Velez, P., Espinosa-Asuar, L., Figueroa, M., Gasca-Pineda, J., Aguirre-von-Wobeser, E., Eguiarte, L. E., Hernandez-Monroy, A., & Souza, V. (2018). Nutrient dependent cross-kingdom interactions: Fungi and bacteria from an

oligotrophic desert oasis. *Frontiers in Microbiology*, *9*(AUG). https://doi.org/10.3389/fmicb.2018.01755

Velez, P., Gasca-Pineda, J., Rosique-Gil, E., Eguiarte, L. E., Espinosa-Asuar, L., & Souza, V. (2016). Microfungal oasis in an oligotrophic desert: diversity patterns and community structure in three freshwater systems of Cuatro Ciénegas, Mexico. *PeerJ*, *4*, e2064. https://doi.org/10.7717/peerj.2064

Visscher, P. T., Dupraz, C., Braissant, O., Gallagher, K. L., Glunk, C., Casillas, L., & Reed, R. E. S. (2010). Biogeochemistry of Carbon Cycling in Hypersaline Mats: Linking the Present to the Past through Biosignatures. In Seckbach Joseph & A. and Oren (Eds.), *Microbial Mats: Modern and Ancient Microorganisms in Stratified Systems* (pp. 443–468). Springer Netherlands. https://doi.org/10.1007/978-90-481-3799-2_23

Wang, B., Adachi, Y., & Sugiyama, S. (2018). Soil productivity and structure of bacterial and fungal communities in unfertilized arable soil. *PLoS ONE*, *13*(9). https://doi.org/10.1371/journal.pone.0204085

Wang, Q., Garrity, G. M., Tiedje, J. M., & Cole, J. R. (2007). Naive Bayesian classifier for rapid assignment of rRNA sequences into the new bacterial taxonomy. *Applied and Environmental Microbiology*, *73*(16), 5261–5267. https://doi.org/10.1128/AEM.00062-07

White, Bruns, T., Lee, S., & Taylor, J. (1990). *White, T. J., T. D. Bruns, S. B. Lee, and J. W. Taylor. Amplification and direct sequencing of fungal ribosomal RNA Genes for phylogenetics* (pp. 315–322).

Wong, H., Ahmed-Cox, A., & Burns, B. (2016). Molecular Ecology of Hypersaline Microbial Mats: Current Insights and New Directions. *Microorganisms*, *4*(1), 6. https://doi.org/10.3390/microorganisms4010006

Zaghouani, M., Kunz, C., Guédon, L., Blanchard, F., & Nay, B. (2016). First Total Synthesis, Structure Revision, and Natural History of the Smallest Cytochalasin: (+)-Periconiasin G. *Chemistry – A European Journal*, *22*(43), 15257–15260. https://doi.org/https://doi.org/10.1002/chem.201603734

Zaitseva, S. V., Abidueva, E. Y., Radnagurueva, A. A., Bazarov, S. M., & Buryukhaev, S. P. (2018). Structure of Microbial Communities of the Sediments of Alkaline Transbaikalia Lakes with Different Salinity. *Microbiology (Russian Federation)*, *87*(4), 559–568. https://doi.org/10.1134/S0026261718040185

Figure legends

Figure 1

(A) The Cuatro Ciénegas Basin within México, and geographic location of Archaean Domes in Pozas Azules Ranch. (B) Detail of an Archaean Domes slice. (C) Domes when the sampling was conducted (note the size scale). Photos by David Jaramillo.

Figure 2

Genera relative abundance of taxa in Archaean Domes, Cuatro Ciénegas Basin sample. A) Bacteria (only showed the most common taxa, more than 1% of diversity) B) Fungi (using Merge database, only fungal ASVs. NA is for ASVs that were not assigned to any genera, but phylum only)

1274
1275 Figure 3
1276 Graphic representation of shared ASVs within Archaean Domes mats sampling
1277 sites. Number of shared ASVs is represented by black bars, showing the exact
1278 number on the top. Dots below bars denote sites where those ASVs are shared, and
1279 lines joining dots indicate the shared sites. Colored bars at bottom left of the main
1280 figure are for ASVs number within each site. Pays show taxonomy of shared ASVs
1281 within all sites (a few but abundant ASVs core).
1282 (A) 16S Archaea and Bacteria, rRNA gene database, (B) Fungi and other Eucarya,
1283 Forward-Only ITS database.
1284
1285 Figure 4
1286 Graph representing null model distribution of Phylogenetic Species Clustering
1287 (nmdPSC) values for all community, abundant and rare taxa from 16S rRNA
1288 database (A) and Forward-Only ITS database (B). Dotted lines are showing
1289 nmdPSC significant values: > +2 is consistent with a sample that had more
1290 phylogenetic overdispersion than expected by chance alone, and nmdPSC value <
1291 -2 indicates more phylogenetic clustering than expected by chance alone; values in
1292 the range +2 and -2 had a null model distribution. nmdPSC values are reported in
1293 Suppl. Table 5.
1294
1295 Figure 5
1296 Pearson correlation analysis within the most common (i.e., involving more than 1%
1297 of diversity) Bacteria, and all genera of Archaea and Fungi (from Merge ITS
1298 database). Colored squares are for significant correlations ($P \leq 0.05$), blue for positive
1299 ones and red for negatives.
1300
1301 Figure 6
1302 Molecular network of soil samples grouped metabolite features into 140 chemical
1303 families. Each node in the network represents one metabolite feature. Nodes
1304 connected to each other are structurally-related (cosine MS^2 similarity score ≥0.7).
1305
1306 Figure 7
1307 Structures of microbial metabolites tentatively annotated in samples S1-S10 (≤ 5
1308 ppm mass error).
1309
1310 Table1
1311 Alpha diversity indices for 16S rRNAgene and Forward-Only ITS region databases
1312 from Archaean Domes CCB microbial mats.
1313
1314 Suppl. Fig. 1
1315 (A) Phylum composition within 16S rRNA gene database (B) Kingdom composition
1316 (based on UNITE database eukaryotic taxonomy) within Forward-Only ITS region
1317 database.
1318
1319
1320

1321 Suppl. Fig. 2
1322 Rarefaction curves for 16S rRNA gene database (A) and ITS region Forward-Only
1323 ITS database (B).
1324
1325 Suppl. Fig. 3
1326 UPGMA dendrogram showing composition similarities among sampling sites
1327 (Forward-Only ITS database for Eucarya UPGMA).
1328 Branch length represent Bray-Curtis and Jaccard-1 dissimilarity coefficient, based
1329 on (A) abundance of 16S rDNA sequences ASVs, and (B) abundance of ITS region
1330 database ASVs. The numbers (height) are Bray-Curtis and Jaccard values.
1331
1332 Suppl. Figure 4
1333 Heatmap analysis showing relative abundance of metabolite features (MS ions in
1334 positive mode) in the Archaean Domes mats samples. On the scale bar, brick red
1335 color indicates increased metabolite levels, and blue color represents decreased
1336 levels. A shows non clustered samples and sites, B clustered samples and sites.
1337
1338 Suppl. Table 1.
1339 List of ASVs Blast hits with <90%, of non-fungal Merge ITS database.
1340
1341 Suppl. Table 2.
1342 Abundance tables (16S rRNA gene and ITS region taxa).
1343
1344 Suppl. Table 3.
1345 Counts of significant negative and positive correlations from Pearson Correlation
1346 Analysis (Figure 5).
1347
1348 Suppl. Table 4.
1349 Tentatively identified microbial metabolites in samples S1-S10 by GNPS and
1350 detailed metabolomic analysis.
1351
1352 Suppl. Table 5
1353 nmdPSC values